

LATE CARBONIFEROUS THIN-SKINNED DEFORMATION IN THE LUBLIN BASIN, SE POLAND: RESULTS OF COMBINED SEISMIC DATA INTERPRETATION, STRUCTURAL RESTORATION AND SUBSIDENCE ANALYSIS

Mateusz KUFRASA*, Agata STYPA, Piotr KRZYWIEC & Łukasz SŁONKA

Institute of Geological Sciences, Polish Academy of Sciences, Twarda 51/55, 00-818 Warsaw, Poland;

e-mails: mateusz.kufrasa@twarda.pan.pl, agata.stypa@twarda.pan.pl,

piotr.krzywiec@twarda.pan.pl, lukasz.slonka@twarda.pan.pl

** Corresponding author*

Kufrasa, M., Stypa, A., Krzywiec, P. & Słonka, Ł., 2019. Late Carboniferous thin-skinned deformation in the Lublin Basin, SE Poland: Results of combined seismic data interpretation, structural restoration and subsidence analysis. *Annales Societatis Geologorum Poloniae*, 89: 175–194.

Abstract: The aim of this study was to investigate the factors, which controlled the lateral change of structural style in the southeastern part of the Lublin Basin (Poland). Five selected seismic reflection profiles were interpreted with a focus on structural interpretation. Along the representative seismic reflection profile, a geological cross-section was constructed and restored. The structural model was supplemented/refined with core analysis to characterize the deformation mode affecting Silurian strata at a sub-seismic scale (i.e. below the seismic vertical resolution). Published palaeothickness maps were used to estimate the pre-deformation thickness of partly eroded Carboniferous rocks. The results of cross-section restoration were then compared to the subsidence modelling carried out for one deep well. The study revealed that during Late Carboniferous shortening, a thick layer of Silurian shales played the role of detachment level, above which brittle Devonian–Carboniferous strata were folded and thrust. The lateral extent of thin-skinned deformation was controlled by the presence of a step in the basement and the pinching out of the Silurian strata. In the northwestern part of the Lublin Basin, the Kock Fault Zone acted as a region of strain concentration, where Silurian shales were tectonically thickened, and shows a ductile style of deformation resembling the mushwad structures of the Appalachian fold-and-thrust belt.

Key words: Quantitative modelling, burial analysis, structural interpretation, Late Carboniferous deformation, Lublin Basin.

Manuscript received 04 December 2018, accepted 4 June 2019

INTRODUCTION

Modern techniques of geological and geophysical modelling are crucial methods of unravelling the structural evolution of sedimentary basins. The Lublin Basin recently was investigated extensively by means of high-quality seismic data calibrated by wells (Krzywiec *et al.*, 2017a, b, 2018b; Tomaszczyk and Jarosiński, 2017). The present authors have focused on the Late Carboniferous deformation preserved in the Lublin Basin (LB) and have constructed a model, based on structural interpretation, cross-section restoration, core analysis and subsidence analysis in order to 1) identify the key factors controlling the Late Palaeozoic style of deformation, 2) characterize the internal structure of the Kock Fault Zone (KFZ), and 3) estimate the initial thick-

ness of the Carboniferous strata. The results derived from seismic interpretation, cross-section restoration, and subsidence analysis in the LB have been published separately for each of these methods (Botor *et al.*, 2002; Krzywiec, 2007, 2009; Tomaszczyk and Jarosiński, 2017). The present study integrates the methods and techniques mentioned above to construct a comprehensive model of the Late Palaeozoic evolution of the LB. The results of 2D seismic interpretation, geological restoration and subsidence modelling were already published in Kufrasa *et al.* (2017) and Stypa *et al.* (2017), but for the purpose of this paper these approaches were supplemented with 3D seismic cube interpretation and core analysis.

GEOLOGICAL SETTING

The study area analysed in this paper is located in SE Poland, within the LB, which is a major Palaeozoic sedimentary basin filled with Ediacaran–Carboniferous strata. It developed above the SW edge of the East European Craton that underwent a complex cycle of basin-forming processes, associated with subsidence, sedimentation and burial of the Palaeozoic sedimentary cover. These processes were punctuated by phases of widespread tectonic deformation that led to basin inversion, thrusting and folding, and associated uplift and ensuing widespread erosion (Figs 1, 2). The Ediacaran-to-Carboniferous history of the cratonic edge in Poland documents the transition from one supercontinent, Rodinia, to another, Pangea. In the Permian–Mesozoic, it formed part of a vast epicontinental basin, i.e., the so-called South Permian Basin, eventually inverted in the Late Cretaceous–Oligocene.

Rifting associated with the break-up of Rodinia led to formation of tectonic half-grabens, filled by a volcano-clastic Neoproterozoic succession, that now are deeply buried beneath the Palaeozoic, Mesozoic and Cainozoic sedimentary cover (Fig. 1). The rift-related Neoproterozoic sedimentary sequence was encountered in SE Poland in several deep research wells (Paczeńska, 2006, 2010, 2014; see also Poprawa, 2006a) and recently was imaged on deep seismic data (Krzywiec *et al.*, 2018a).

After this regional rifting event, the Tornquist Ocean developed and separated the two continental plates – Baltica and Amazonia – born out of Rodinia (Fig. 1B). The Cambrian–Ordovician sedimentary succession of the East European Craton in Poland, characterized by rather minor and gradual lateral changes in thickness caused by relatively steady subsidence, was deposited along the passive margin of this ocean (Poprawa, 2006a). Regional subsidence pattern changed in the latest Ordovician–earliest Silurian, when the Caledonian thrust belt was emplaced over the cratonic edge, and resulted in rapid subsidence within Caledonian foredeep basin and deposition of a syn-tectonic fine-grained, shaly Silurian succession above the SW edge of the East European Craton (cf. Poprawa, 2006b; Mazur *et al.*, 2016). The evolution of the Caledonian foredeep basin continued until the Early Devonian (Figs 1, 2).

A large part of the cratonic edge underwent substantial uplift following the Devonian sedimentation. This uplift might have been related to the geodynamic processes acting within the interior of the East European Craton, e.g. in the Pripyat–Dnipro–Donetsk Basin (Fig. 1E). During this so-called Bretonian tectonic phase, large crustal blocks were uplifted along deeply rooted reverse faults. This tectonic phase was followed by regional erosion that removed part of the pre-Carboniferous sedimentary cover and formed a regionally extensive unconformity (cf. Krzywiec *et al.*, 2017b).

The next phase of geological evolution of the study area started with deposition of the Carboniferous sedimentary succession within the sedimentary basin that had been formed at the distal Variscan foreland (Narkiewicz, 2007). Variscan (latest Carboniferous) tectonic movements led to the formation of a thin-skinned fold-and-thrust belt verg-

ing toward the NE and emplaced above the cratonic edge in SE Poland, first proposed by Antonowicz *et al.* (2003), and recently imaged on a deep seismic reflection profile (Krzywiec *et al.*, 2017a, b). It involves Ediacaran–Devonian/Carboniferous deposits in its more internal part (the Radom–Kraśnik Block) and Silurian–Carboniferous deposits in the most external part, i.e. within the LB, where the study area is located (Figs 1F, 2). The Variscan collisional event completed the formation of the Pangea supercontinent. It was fragmented during widespread Permian–Cretaceous and younger rifting. In western and central Europe, the Pangea break-up led to the formation of the so-called Central European Basin System (Ziegler, 1990; Scheck-Wenderoth *et al.*, 2008; Pharaoh *et al.*, 2010). The Polish Basin, together with the part of it that is currently located in SE Poland, formed the easternmost part of this Permian–Cretaceous system of epicontinental basins. After the Permian rifting, the Polish Basin experienced long-term thermal subsidence, starting in the Permian and lasting until the Late Cretaceous. This long-term subsidence was punctuated by Zechstein (Wuchiapingian)-to-Scythian (Olenekian), Oxfordian-to-Kimmeridgian, and early Cenomanian major pulses of accelerated, tectonic subsidence (Dadlez *et al.*, 1995; Stephenson *et al.*, 2003). In SE Poland, Late Jurassic (earliest Oxfordian) and earliest Late Cretaceous (Cenomanian) regional uplifts associated with widespread erosion were documented recently, using newly acquired regional seismic profiles (Krzywiec *et al.*, 2018b).

After prolonged Permian–Cretaceous subsidence, the Polish Basin ceased to exist, owing to the Late Cretaceous–Palaeogene inversion that, in its SE segment, started in the late Turonian and lasted until Maastrichtian–post-Maastrichtian times (Krzywiec, 2009; Krzywiec *et al.*, 2009). The inversion tectonics was associated with significant uplift and erosion of the axial part of the Polish Basin as well as substantial syn-tectonic sedimentation along the flanks of uplifted, inverted structures (Krzywiec *et al.*, 2009; Remin *et al.*, 2016; Krzywiec *et al.*, 2018b).

DATA AND METHODOLOGY

Seismic data interpretation: general methodology and available data

Five 2D seismic-reflection profiles of total length 240 km and one 3D seismic cube covering an area of 213 km² (for location see Fig. 2) were interpreted in order to investigate geometry and kinematics of the Late Palaeozoic structures in the LB. These data were shared by the National Geological Archive and Polish Oil and Gas Company within the GAZGEOLMOD research project aimed at unravelling tectonostratigraphic evolution of the southwestern edge of the East European Craton. Interpretation of the 3D seismic survey allowed investigation of the geometric relations between the main (first-order) and subordinate (second-order) folds and thrusts. Most of the interpreted profiles are perpendicular to the NW–SE-striking first-order structures within the LB. In order to highlight differences in structural style, the Lublin Basin was subdivided into northwestern and southeastern parts (red dashed line on Fig. 2). The divi-

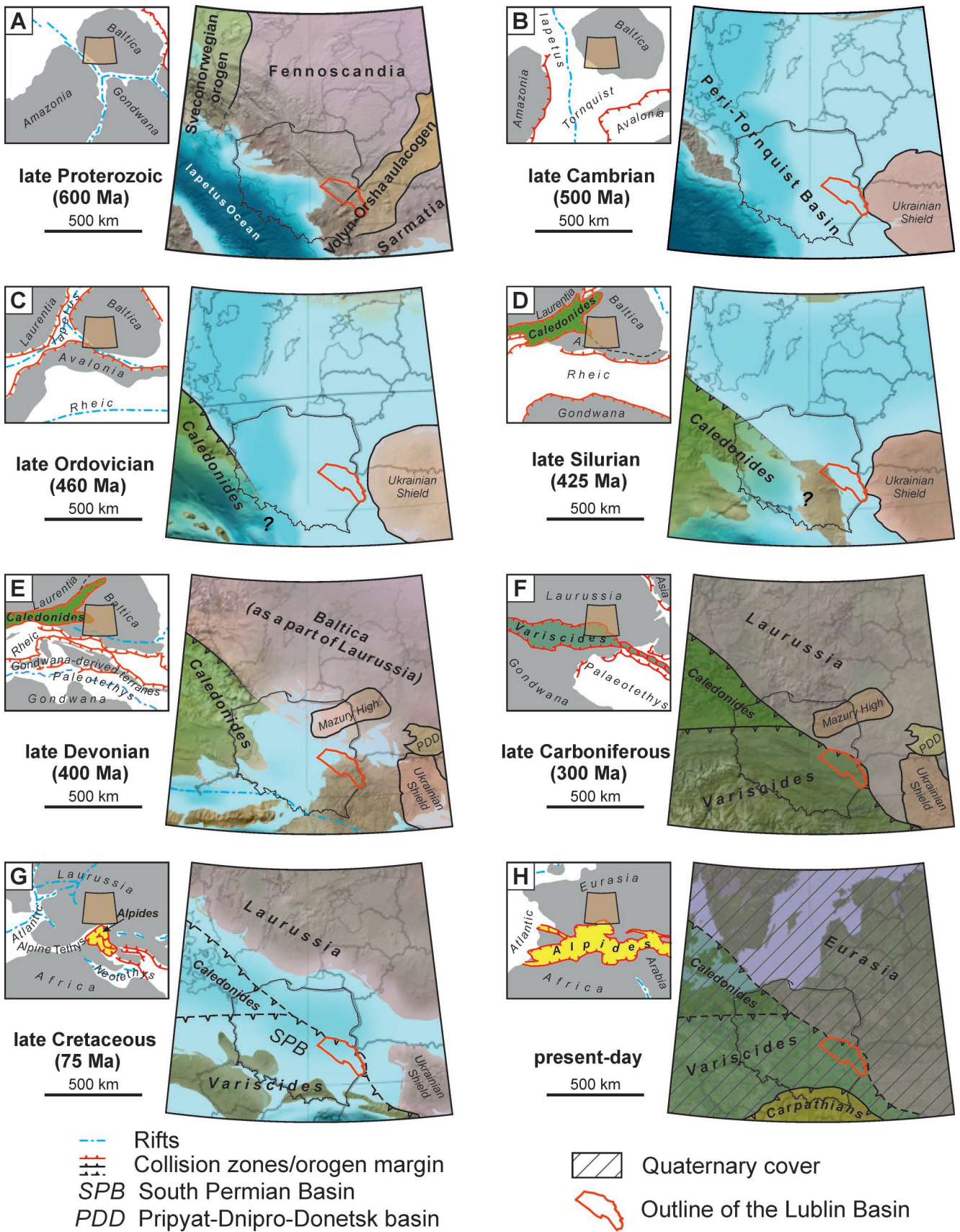


Fig. 1. Set of maps showing configuration of palaeocontinents, rifts and collision zones. Orange box on each inset map indicates detail from the main structural units in the area of Poland. See text for details. Source maps (Deep Time Maps, 2019) were supplemented with information taken from Kusznir *et al.* (1996), Nikishin *et al.* (1996), Stovba and Stephenson (1999), Bogdanova *et al.* (2008), Schmid *et al.* (2008), Stampfli *et al.* (2013)

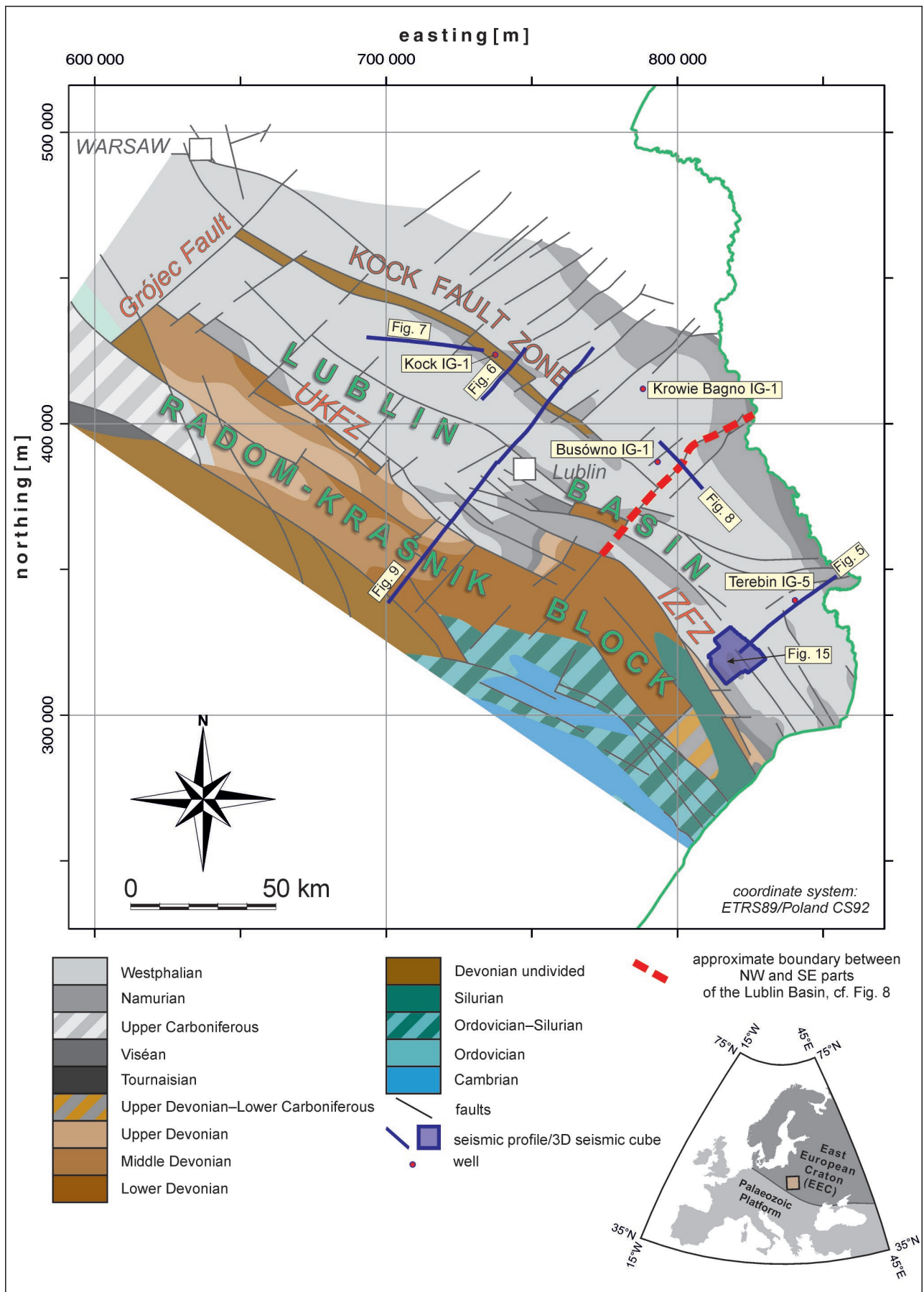


Fig. 2. Geological map of the study area without the Permian–Mesozoic and Cainozoic cover (Pożaryski and Dembowski, 1983), showing the location of seismic lines and wells used in this study. UKFZ – Urszów–Kazimierz Fault Zone, IZFZ – Izbica–Zamość Fault Zone. One of the seismic reflection profiles was depth-converted and restored (see Fig. 9). Figure taken from Kufrasa *et al.* (2017).

sion line is at the SE termination of the Kock Fault Zone – a major basement step that significantly influenced the entire Palaeozoic evolution of the LB (cf. Antonowicz *et al.*, 2003; Antonowicz and Iwanowska, 2004; Krzywiec *et al.*, 2017b; Tomaszczyk and Jarosiński, 2017).

Nine regional seismic horizons were interpreted. The structural interpretation was carried out with the aid of

the IHS Kingdom software (IHS Kingdom, 2019). These horizons were tied to stratigraphic boundaries using two synthetic seismograms constructed for deep wells that penetrated the Palaeozoic sedimentary cover (Fig. 3). The seismic wavelet used in synthetic seismogram construction was extracted from seismic lines localized in the vicinity of the deep wells; the synthetic seismograms were construct-

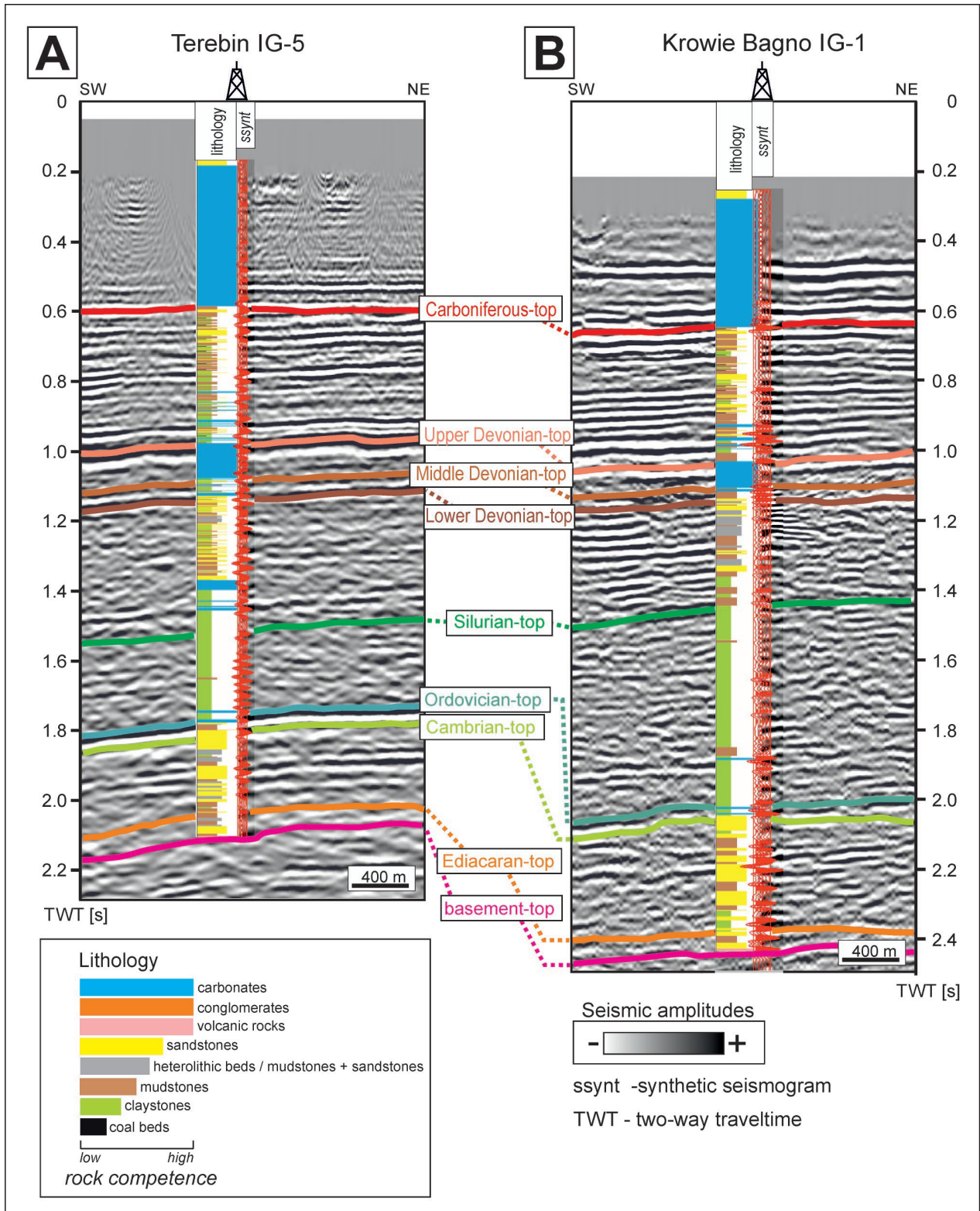


Fig. 3. Synthetic seismograms constructed for the northwestern (A) and southeastern part of the Lublin Basin (B); note correlation between rock competency and seismic amplitude. For the location of the wells see Figure 2.

ed with the use of CGG Hampson Russell software (CGG, 2019). The depth-converted, interpreted, regional, seismic profile was used for sequential restoration.

Geological cross-section restoration

One seismic reflection profile was restored sequentially with the use of MOVE software provided by Midland Valley and Petroleum Experts (Move, 2019). The quantitative analysis of a cross-section requires a plane strain state to reduce the effect of material movement away from the plane of the cross-section (Woodward *et al.*, 1989). Thus, the geological cross-section selected for restoration in this study is oriented SW–NE, parallel to the main direction of regional tectonic transport and perpendicular to the strike of the Late Carboniferous folds and thrusts (Fig. 2). Contraction of the sedimentary cover causes shortening of the strata, decoupled along a regional decollement. For this analysis, the authors divided the sedimentary cover into brittle and ductile complexes and used the assumption of Thomas (2001, 2007a), where competent and incompetent layers were restored, assuming constant line length and constant cross-sectional area, respectively. The pin line is located, where the sedimentary cover remains undeformed during restoration; in the present case study, it is placed beyond the lateral extent of the Carboniferous deformations, NE of the Lublin Basin. The predeformation thickness of the stratigraphic units was based on the lithofacies and original thickness maps of Modliński (2010) for the Palaeozoic rocks and estimated by means of the vertical distance between sea level and the intersection of palaeoisopachs with the cross-section plane, which was projected onto the base of a given stratigraphic unit (Fig. 4).

Subsidence analysis

1D subsidence analysis (backstripping) was conducted for the Busówno IG-1 well using the BasinMod 2014 software (BasinMod, 2019). This well was chosen because of its proximity to the seismic profile analysed as well as the availability of the data required for modelling, which was insufficient in other wells. The modelling relied on published well data and information available from the Central Geological Database (Central Geological Database, 2019) and was supplemented with the results of seismic data interpretation. Using all this information, the Phanerozoic sedimentary infill was divided into stratigraphic units, each with an assigned thickness and lithology, as well as numerical ages defining the time interval between its lower and upper boundaries. Numerical ages were assigned using the stratigraphic chart of Gradstein *et al.* (2012). The modelling employed a decompaction correction based on the algorithm of Baldwin and Butler (1985), whilst the main petrophysical parameters used in the decompaction procedure were the initial porosity and compaction factors characteristic for a given lithology. For selected stratigraphic units characterized by mixed lithological composition, new lithological units were defined on the basis of the percentage of primary lithological ingredients.

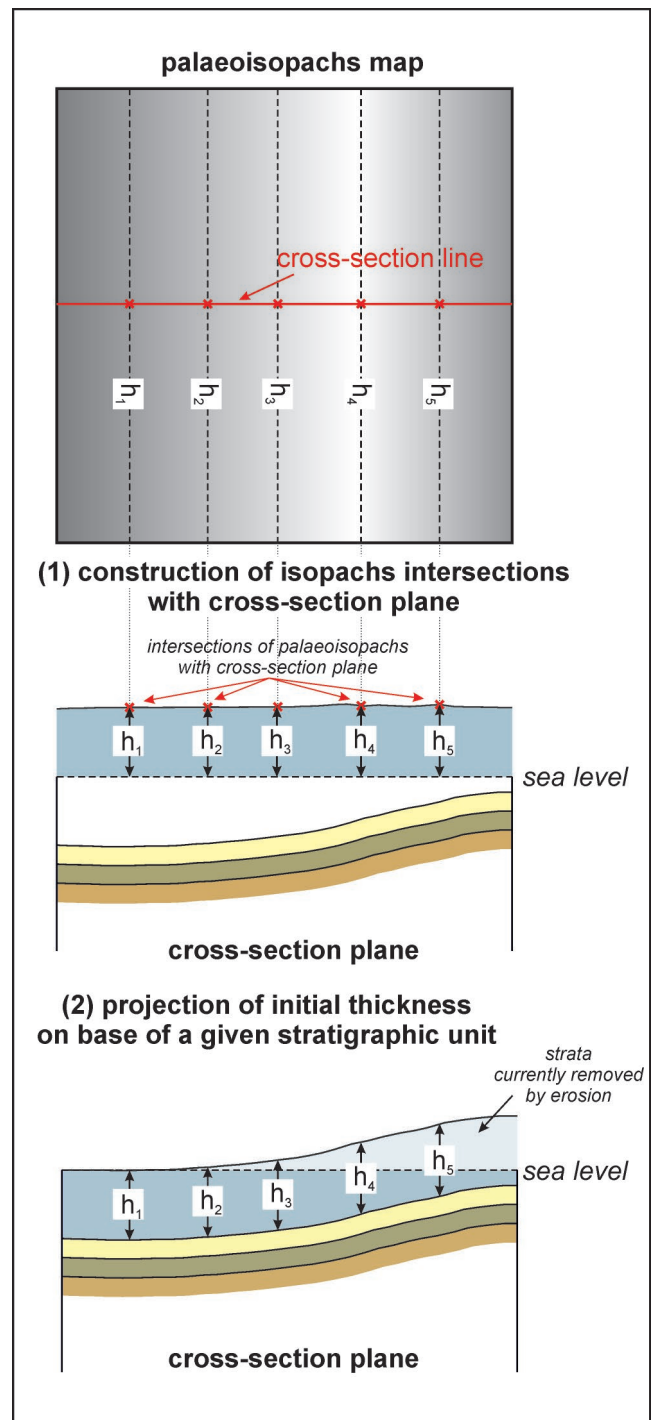


Fig. 4. Cartoon illustrating projection of palaeoisopachs on a cross-section plane in order to construct the pre-deformation thickness of a given lithostratigraphic unit.

The subsidence analysis was applied to quantify the extent of the erosion, which took place after the phases of regional uplift. The analysis was performed, relying on two opposing scenarios that employed different variables. In the first scenario, the thickness of eroded sediments according to Modliński (2010) and heat flow changes were assumed for calibration of the models. In the second scenario, a constant heat flow and changes in the thickness of the eroded Devonian and Upper Carboniferous strata were assumed.

Both scenarios were calibrated using vitrinite reflectance data (%Ro), published by Paczeńska (2007). The depth of the top of the basement was determined by integrating the seismic data and the well profile was extended accordingly.

SEISMIC DATA INTERPRETATION

The Carboniferous strata are characterized by the occurrence of discontinuous reflections, resulting from rapid facies changes (Dziewińska and Józwiak, 2000). The top of the Palaeozoic sedimentary sequence is marked by an uneven surface of angular unconformity, separating these rocks from the overlying Permian–Mesozoic strata (Figs 5–9). Krzywiec *et al.*, (2017a, b, 2018b) provide more details and additional seismic examples. Distinct reflections are related to the tops of sandstone and limestone layers in the upper and lower parts of Carboniferous (Fig. 3), respectively. The limestone layers previously were recognized as regional marker horizons (Kaczyński, 1984). The erosional unconformity that separates the Carboniferous from Devonian or older strata, the so-called Bretonian unconformity (cf. Krzywiec *et al.*, 2017a, b), is marked by an abrupt increase in P-wave velocity (Fig. 3; Bilowa, 1981). A series

of high-amplitude reflections within the pre-Carboniferous strata is related to the Middle Devonian and Ordovician carbonates (Fig. 3; Pepel, 1974; Bilowa, 1981). The lowest reflectors mark a velocity discontinuity at the basement-cover interface (Fig. 3).

The intensity/amplitude of seismic reflection is dependent on mechanical rock properties, which in turn depend on the lithological composition. In this study, the Palaeozoic sedimentary cover of the LB is generally considered to be brittle, apart from the thick, fine-grained Silurian strata, which played the role of regional detachment layer for the Variscan (i.e. latest Carboniferous) tectonic deformations (Fig. 5; Antonowicz *et al.*, 2003; Krzywiec *et al.*, 2017a, b; Tomaszczyk and Jarosiński, 2017). The basal detachment level in the Lublin Basin is located within the thick sequence of fine-grained Silurian shales and mudstones (Krzywiec *et al.* 2017a, b; Tomaszczyk and Jarosiński, 2017). Variation in the lithological composition of the sedimentary rocks is responsible for differences in the mode of strain accommodation: brittle layers (sandstones, limestones) tend to crack, while ductile strata (shales, marls, evaporites) deform by folding or distributed shear, as described in the following chapter.

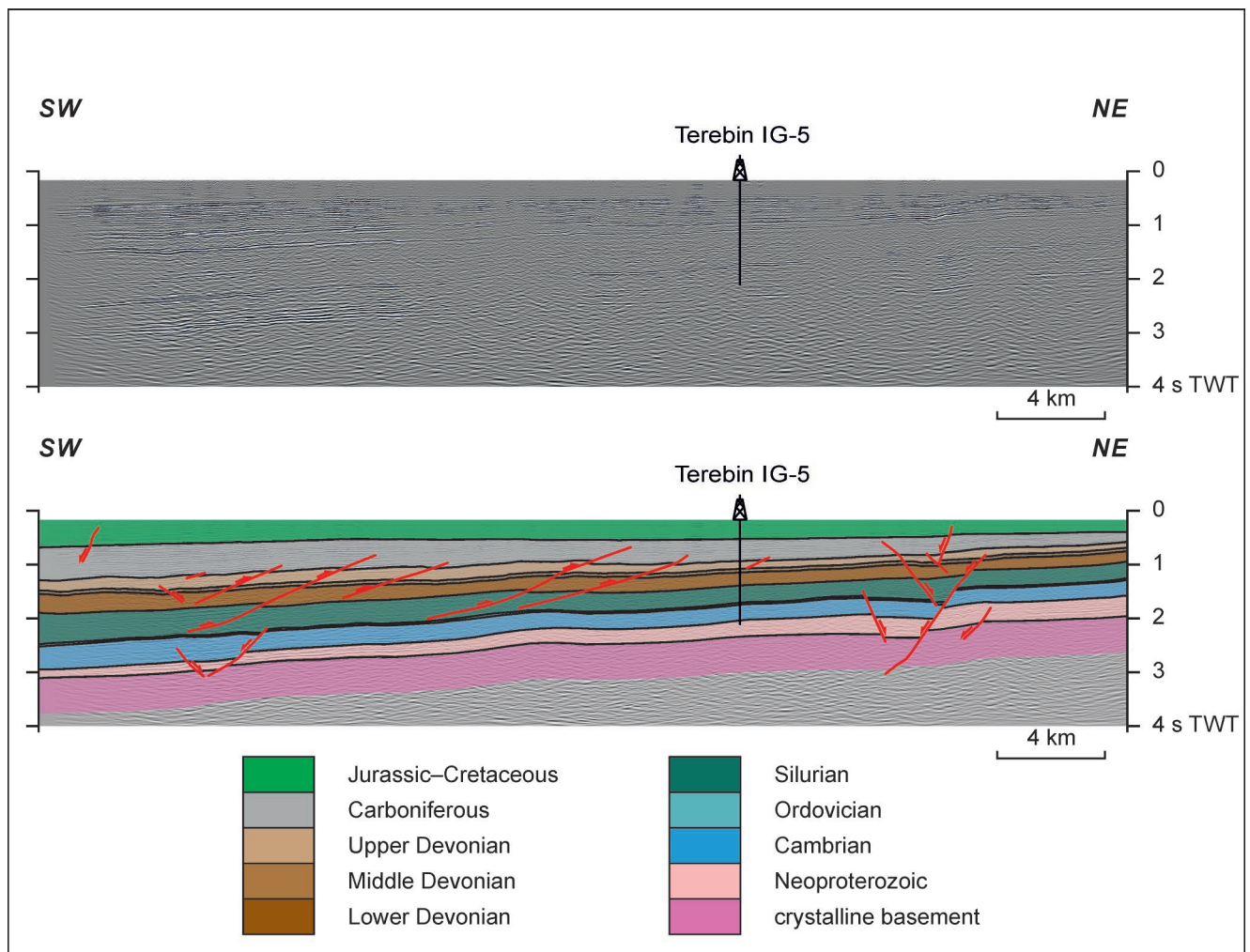


Fig. 5. Uninterpreted (top) and interpreted (bottom) seismic line showing thrusts cutting the Palaeozoic strata in the SE part of the Lublin Basin. See Figure 2 for location. Figure taken from Kufraśa *et al.* (2017), modified.

STRUCTURAL INTERPRETATION AND MODELING

The structural style is characterized by NW–SE-striking folds and thrusts that deform the wedge-shaped Palaeozoic sedimentary cover of the LB (Figs 5–6); these deformations were generated during the Late Carboniferous (Variscan orogeny). The structures usually show a forelandward vergence (i.e. towards the northeast), although opposite-verging deformations are found as well. In the southeastern part of the LB, a few normal faults were found, striking northwest-southeast and cutting the crystalline basement and the Palaeozoic–Mesozoic sedimentary cover (cf. Krzywiec, 2009; Kufraśa *et al.*, 2018). The intensity of deformation decreases towards the northeast, i.e. towards the interior of the East-European craton, where the thrusts become scarce and less prominent (Fig. 5).

The northwestern part of the Lublin Basin is characterized by significant lateral thickness changes of the Silurian–Carboniferous sedimentary cover that reaches up to 8 km in thickness near the southwestern termination of the basin, in contrast to 5 km in the northeastern part (see Krzywiec *et al.*, 2017a; Mazur *et al.*, 2018). The Kock Fault Zone (KFZ) is one of the most prominent tectonic structures in this part of the basin (Figs 2, 6). The KFZ is a NW–SE-striking basement step, related to a high-angle reverse fault that cuts the basement and the Lower Palaeozoic strata, and overlain by the products of thin-skinned Variscan thrust deformation (Antonowicz *et al.*, 2003; Antonowicz and Iwanowska, 2004; Krzywiec *et al.*, 2017b; Tomaszczyk and Jarośniński, 2017). The thin-skinned anticline appears to have been detached within the thick Silurian fine-grained shale complex and its core is made of structurally thickened mudstones and siltstones. These structures resemble mush-

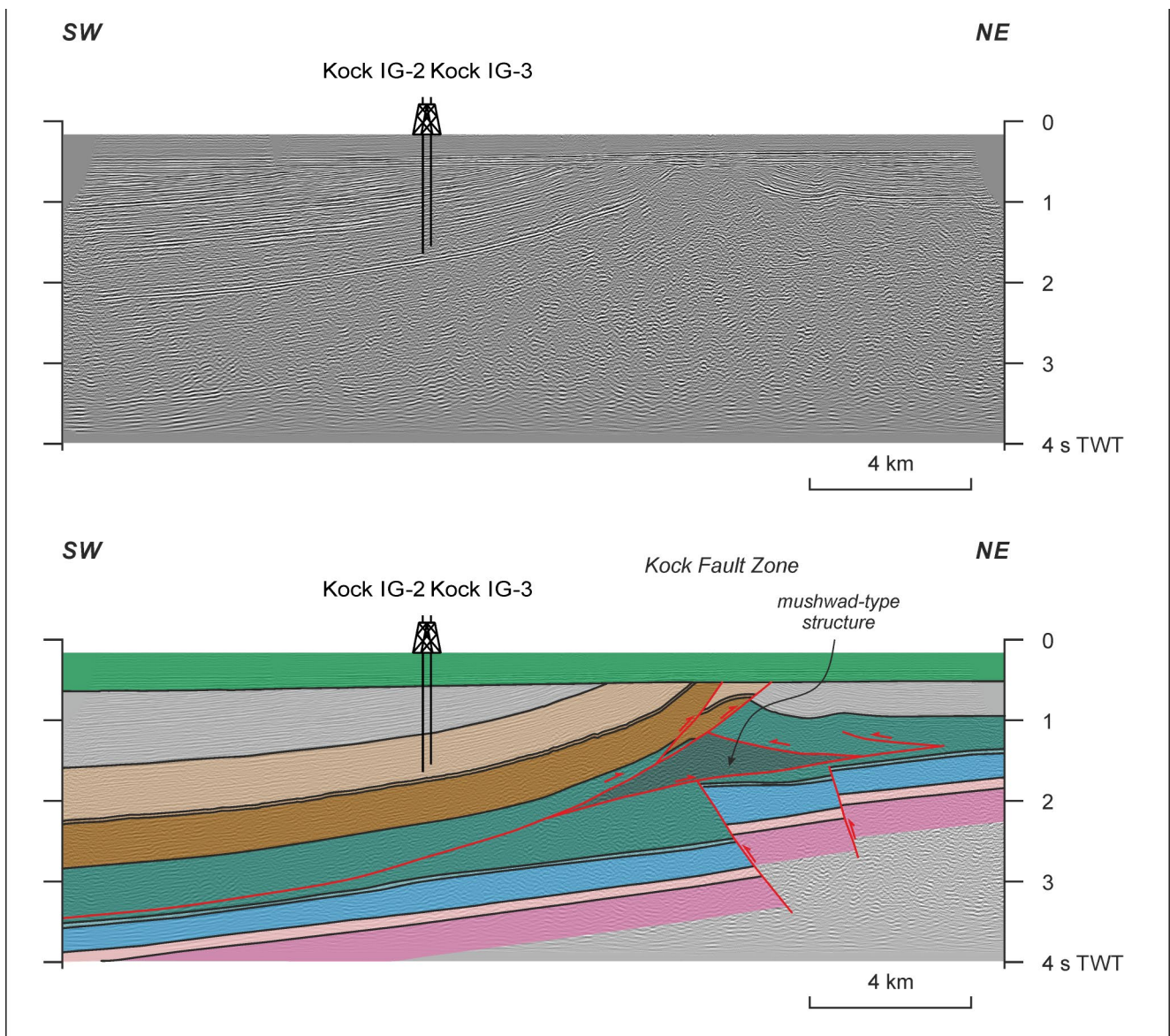


Fig. 6. Uninterpreted (top) and interpreted (bottom) seismic line showing thin-skinned compressional Late Carboniferous deformations developed above the basement step, Kock Fault Zone. See Figure 2 for location and Figure 5 for stratigraphic code. Figure taken from Kufraśa *et al.* (2017), modified.

wad-type structures, similar to those reported in the Appalachians (Thomas, 2001, 2007a, b; Krzywiec *et al.*, 2017b; see discussion). Thickness reduction of the Upper Devonian strata above the KFZ can be observed and it testifies to the activity of this fault during the Late Devonian (Fig. 7). The hanging wall of the KFZ consists of tectonic blocks, bounded by NE-striking, high-angle, mostly reverse faults, which cut the basement and the pre-Carboniferous sedimentary sequence. Late Devonian hanging wall uplift in the KFZ resulted in erosion, which locally reached the Silurian strata (Figs 8, 9; Krzywiec *et al.*, 2017b; Kufraśa *et al.*, 2018).

The occurrence of the Late Palaeozoic thin-skinned structures in the northwestern part of the LB is restricted to the area between the KFZ and the UKFZ (Fig. 2), where both fore- and hinterland-vergent structures cut the Silurian–Carboniferous strata (Fig. 9). These are mostly fault-related folds, cut by fore- and backthrusts (Narkiewicz *et al.*, 2007a; Krzywiec, 2009; Tomaszczyk, 2015; Krzywiec *et al.*, 2017b). The thrusts dip at angles ranging between 30° and 60° and terminate in the Carboniferous strata (Figs 6, 9). The occurrence of faults abutting against the Silurian strata is confined to the KFZ. It is possible that these thrusts

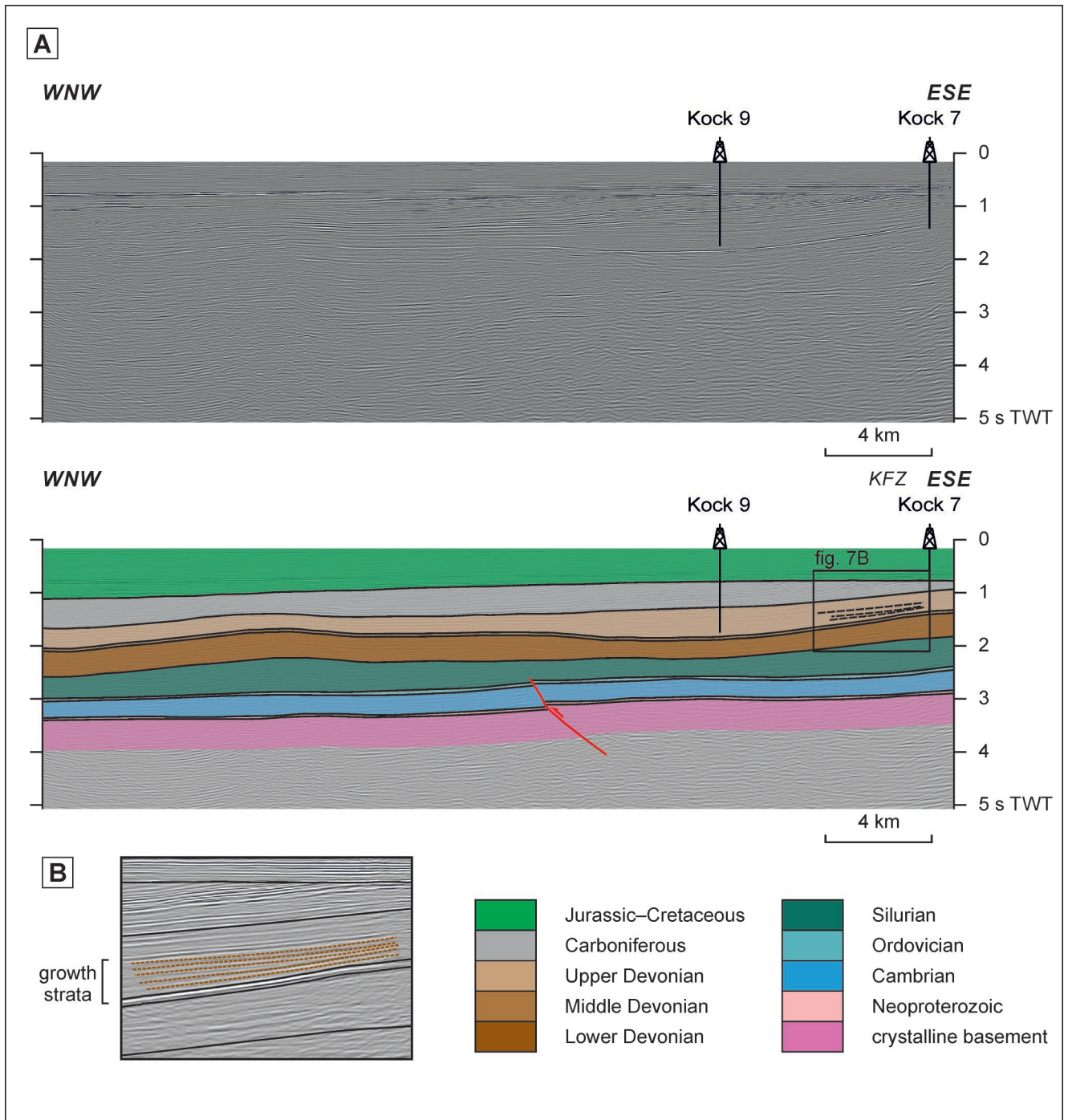


Fig. 7. Details of the Kock Fault Zone (KFZ). **A.** Uninterpreted (top) and interpreted (bottom) seismic line showing thickness reduction of the Upper Devonian strata in the vicinity of the KFZ pointing to the syndepositional activity of this structure. **B.** Detail from Upper Devonian growth strata; see Figure 2 for location. Figure taken from Kufraśa *et al.* (2017), modified.

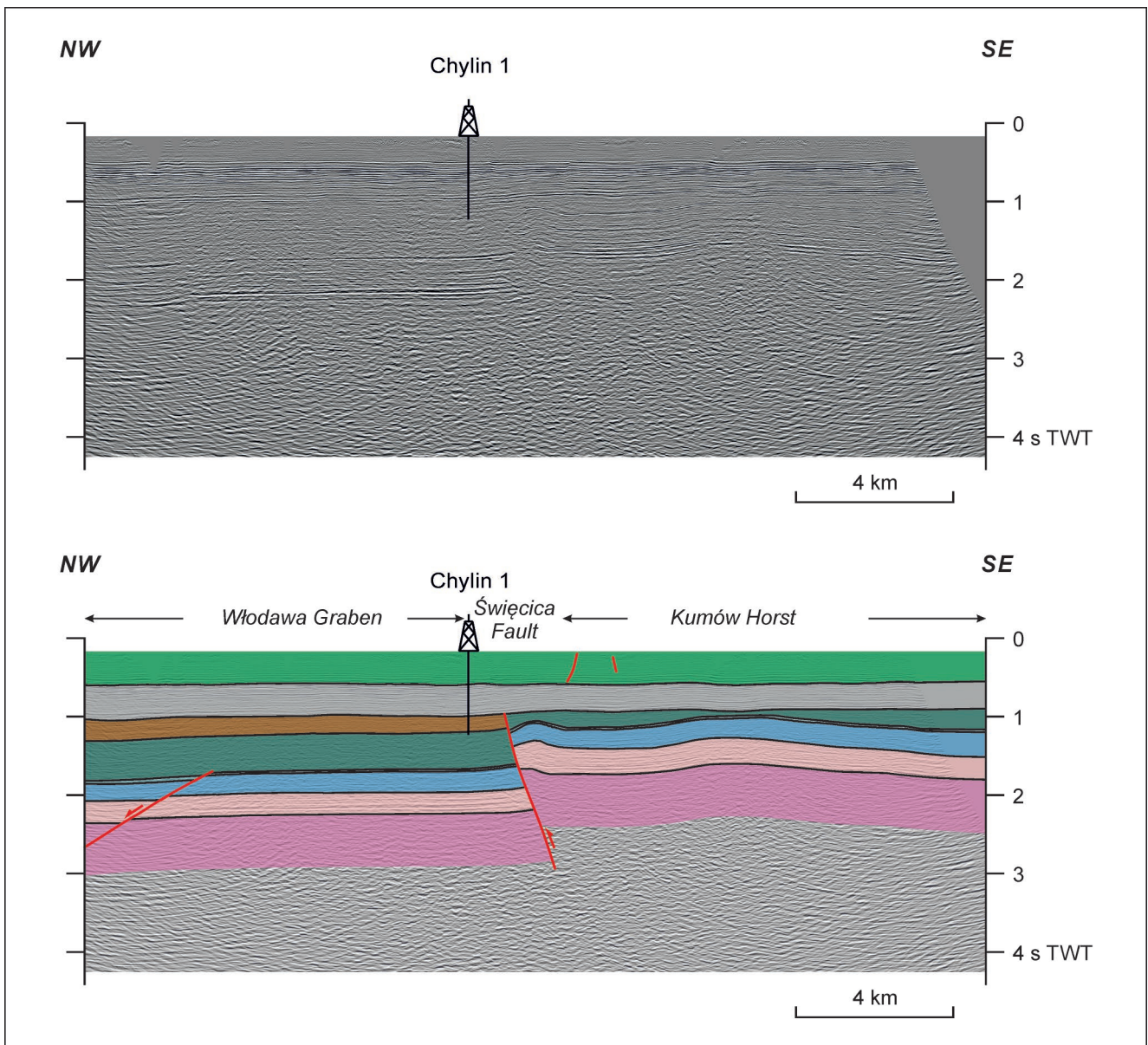


Fig. 8. Uninterpreted (top) and interpreted (bottom) seismic line showing high-angle reverse fault in the hanging wall of the KFZ. See Figure 2 for location and Figure 5 for stratigraphic code. Figure taken from Kufrasa *et al.* (2017), modified.

multiply the Silurian rocks within a duplex resembling a mushwad-type structure (Fig. 6). However, recognizing the internal structure of the mushwad remains difficult owing to the poor quality of seismic data in this region. The opposite vergence of folds in the hanging wall and the footwall of the KFZ may indicate the occurrence of both fore- and backthrusts (Fig. 6). These faults would have been propagated coevally and accommodate the Late Carboniferous shortening. The abutting of these thrusts in Silurian strata may be explained with the aid of mechanical stratigraphy, as fault propagation through ductile material is inhibited, owing to the increased plasticity of the fine-grained rocks.

The lateral variation in vertical throw within the KFZ seems to control the position of the mushwad-type structure relative to the basement step. These along-strike fluctuations in the KFZ already have been reported by Krzy-

wiec *et al.* (2017b). Where the fault offset does not exceed ~1,700 m (0.7 s), the triangular zone of intensive deformation is located above the basement fault (Fig. 6). For higher fault offsets, the zone of increased strain concentration developed in front of the basement fault (Fig. 9).

The geometric and kinematic admissibility of the Variscan structures was tested by means of sequential restoration, consisting of four steps (Fig. 9). Late Carboniferous folds and thrusts occur mostly in the area, flanked by the Radom–Kraśnik Block and the KFZ (Fig. 9A). Flattening of the Variscan unconformity surface was followed by the reconstruction of the pre-deformation and pre-erosion thickness of the Carboniferous strata on the basis of published maps (Fig. 9B). This exercise showed that from 200 up to 2,000 m of the uppermost Carboniferous sedimentary rocks were removed by Variscan erosion. This value probably was higher in the areas characterized by

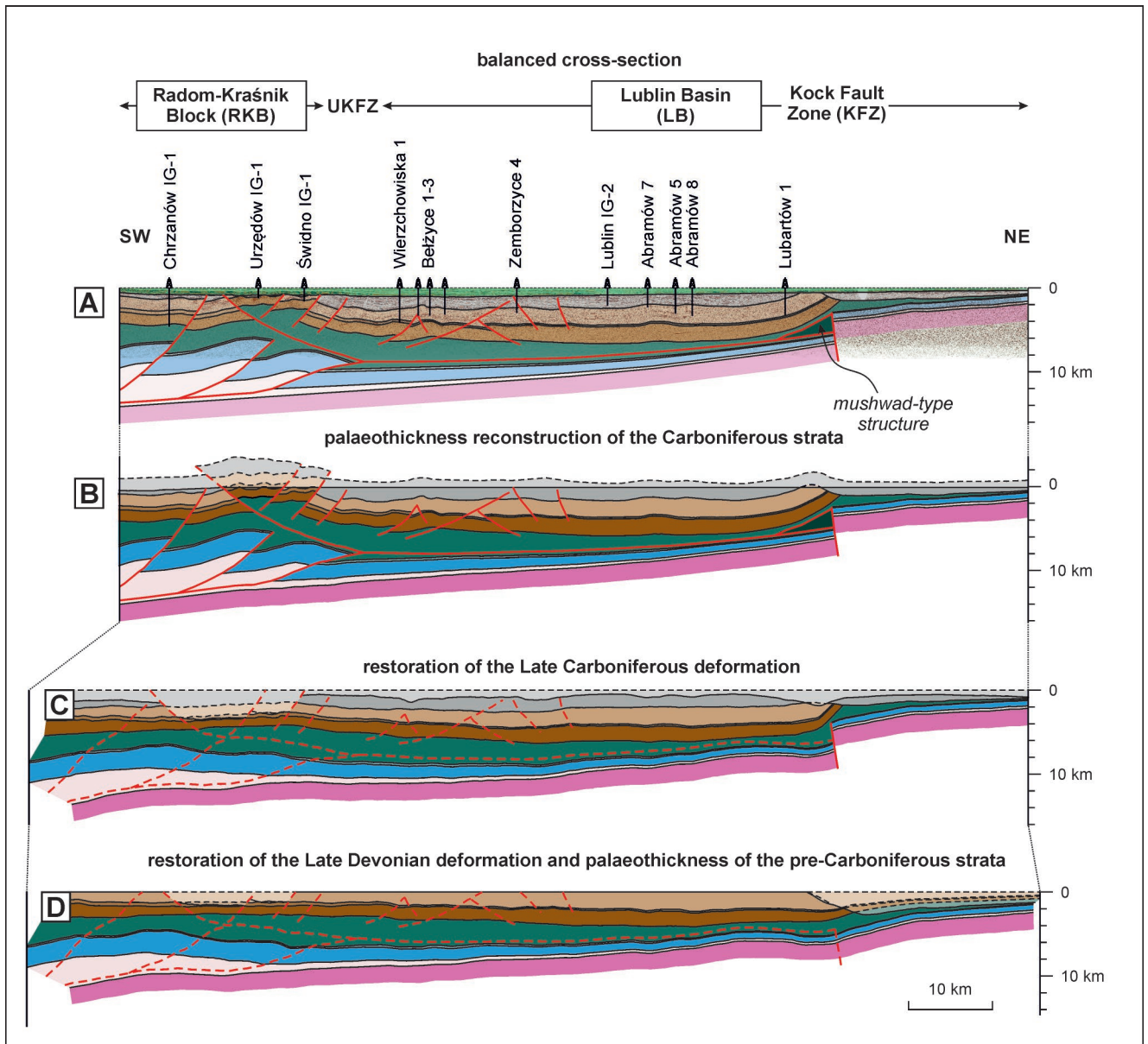


Fig. 9. Sequential restoration for the regional seismic line. Initial thickness of Palaeozoic strata, derived from pre-deformation thickness based on the maps of Modliński (2010), is marked by dashed line and pale colours; UKFZ – Ursynów-Kazimierz Fault Zone. Figure taken from Kufraśa *et al.* (2017), modified.

significant folding and thrusting, i.e. the KFZ and SW margin of the LB, where the entire Carboniferous sequence is missing (Fig. 9B). About 10 km of difference in horizontal length between the deformed and undeformed Carboniferous strata is regarded as the minimum amount of Variscan shortening (compare Fig. 9B, C). The Late Devonian basement faulting within the KFZ resulted in up to 3,000 m of erosion in its hanging wall (Fig. 9D). The shortening associated with this event did not exceed 500 m, although the fault displacement was more than 2,500 m. The predominance of the vertical throw component over the horizontal shortening is characteristic for slip along a high-angle fault without folding, where the strain is accommodated mostly by vertical uplift.

SUBSIDENCE MODELLING

1D modelling of the tectonic subsidence and burial history was performed for the Busówno IG-1 well (see Fig. 1 for location) to determine the extent of erosion of the Middle and Upper Devonian and Upper Carboniferous strata. The results allowed the delineation of four main episodes of increased subsidence (Neoproterozoic–Early Ordovician, Middle Ordovician–Silurian, Devonian–Carboniferous and Late Cretaceous) as well as two stages of uplift and erosion taking place in the Late Devonian–Early Carboniferous and Late Carboniferous–Late Permian (Fig. 10).

In scenario 1 (Fig. 11), the original (pre-deformation and pre-erosion) thicknesses of the eroded Devonian (Middle

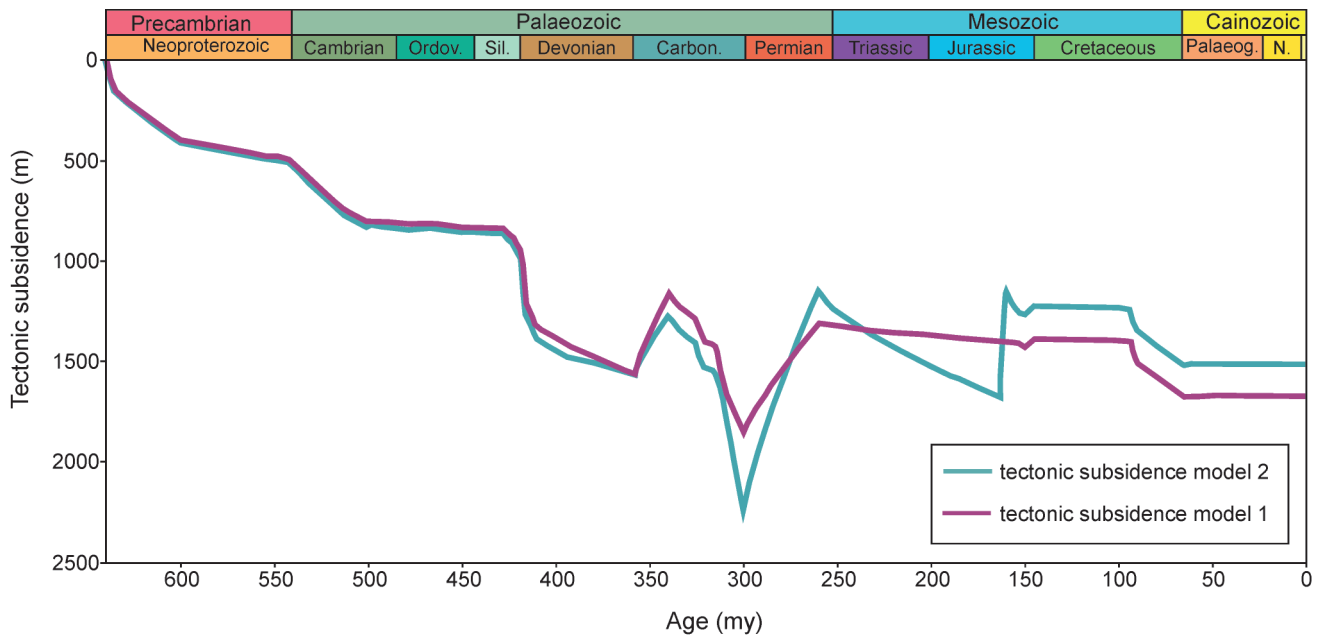


Fig. 10. Tectonic subsidence curves for scenario 1 (pink line) and scenario 2 (green line) for the Busówno IG-1 well. Figure taken from Stypa *et al.* (2017).

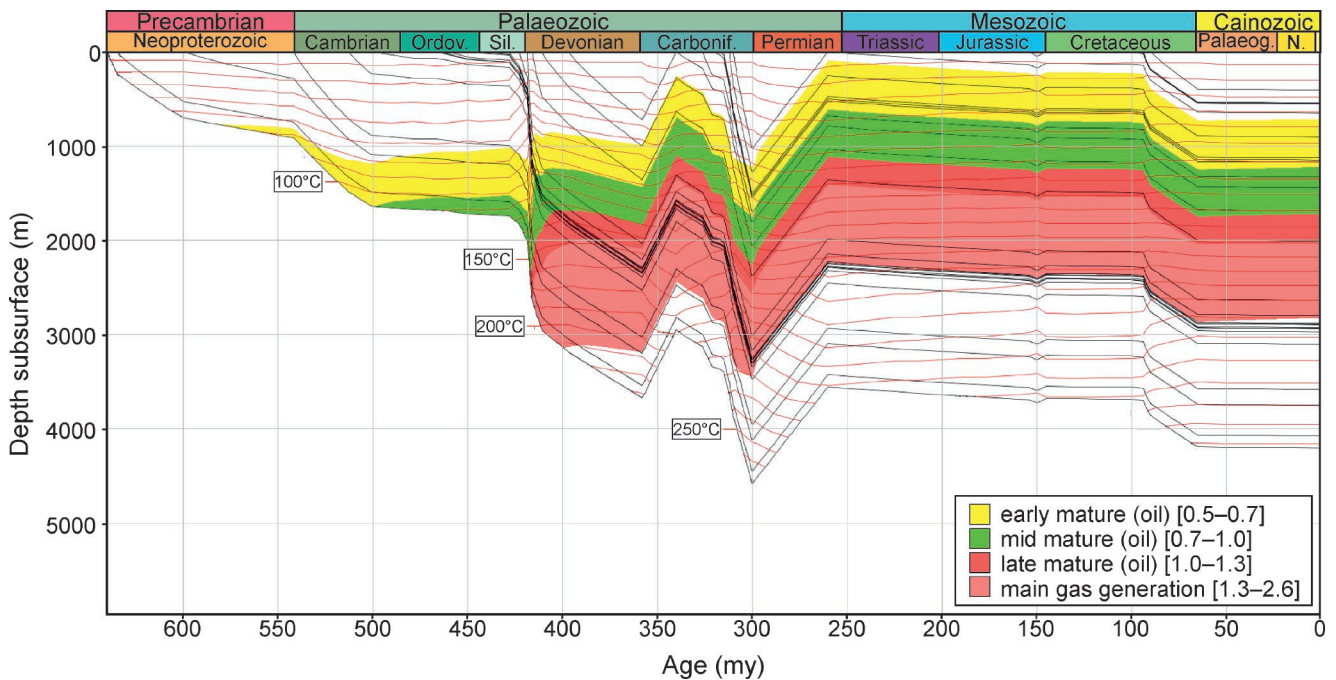


Fig. 11. Scenario 1 of the burial history for the Busówno IG-1 well. Black lines – burial graphs for each stratigraphic unit; red lines – isotherms each with an assigned temperature ($^{\circ}\text{C}$) value. Figure taken from Stypa *et al.* (2017).

and Upper Devonian – 724 m) and Carboniferous (Upper Carboniferous – 1,025.9 m) were derived from the regional thickness maps of Modliński (2010); the stratigraphic, lithological, petrophysical and thermal maturity data after Paczeńska (2007) were used. The present-day heat flow for the Busówno IG-1 is 48 mW/m^2 (Paczeńska, 2007). The model was calibrated using vitrinite reflectance data, comprising 24 measurements from upper Viséan–Westphalian and Ediacaran–Lochkovian strata (Paczeńska, 2007). In order to achieve acceptable calibration, it was necessary to

assume a significantly higher heat flow (90 mW/m^2) than is observed today. However, even when such assumptions were made, the calibration of the model was not satisfactory, as the calculated maturity curve was incompatible with the maturity data that had been measured (%Ro).

In scenario 2 (Fig. 12), a constant heat flow (63 mW/m^2) was assumed and model calibration was achieved by testing different thicknesses of eroded Devonian and Upper Carboniferous strata. The best fit to the measured data was obtained by applying 500 m of Middle and Upper Devoni-

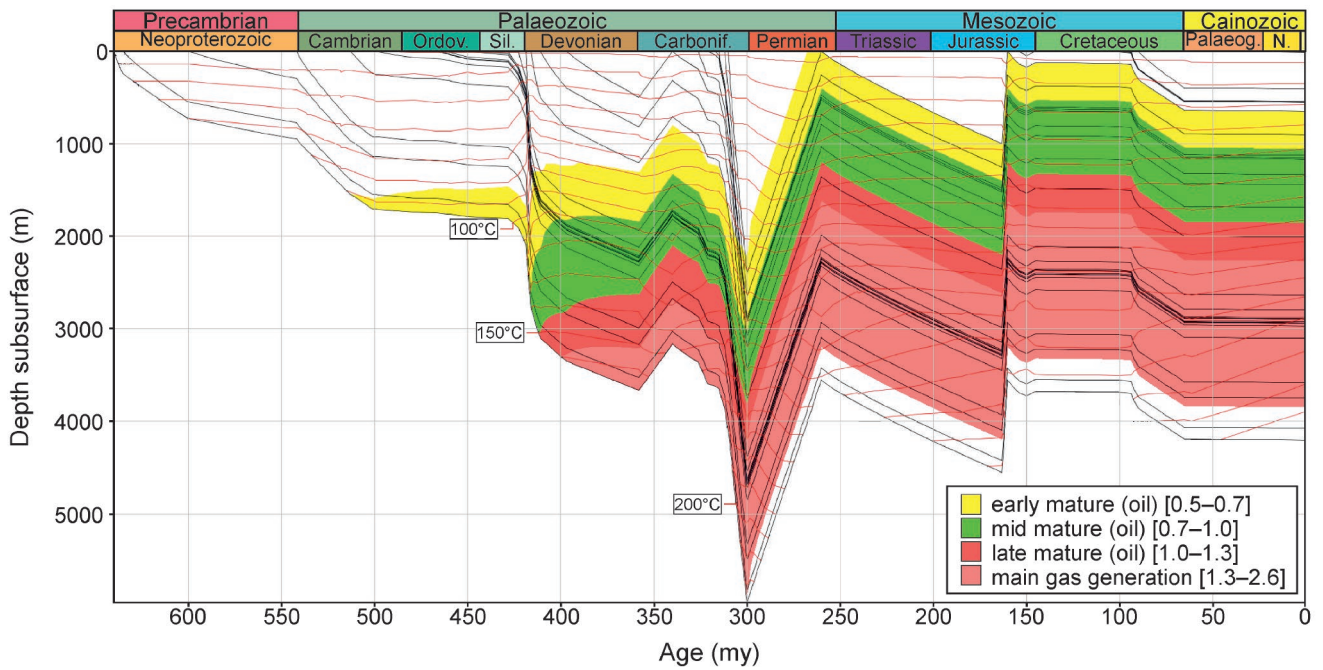


Fig. 12. Scenario 2 of the burial history for the Busówno IG-1 well. Black lines – burial graphs for each stratigraphic unit; red lines – isotherms each with an assigned temperature ($^{\circ}\text{C}$) value. Figure taken from Stypa *et al.* (2017).

an, 2,400 m of Upper Carboniferous and 1,000 m of Triassic–Jurassic strata. Petrophysical, stratigraphic, lithological, and thermal maturity data also were obtained from Paczeńska (2007). In this scenario, a very good fit with the calibration data was achieved (Fig. 13). Therefore, scenario 2 was selected as being much more viable, since better results were obtained on the basis of more realistic assumptions.

The results of subsidence analysis suggest that increased Devonian–Carboniferous subsidence influenced the most the thermal maturity of the basin sedimentary infill, which is compatible with the results of other studies in this area (Narkiewicz, 2003, 2007; Narkiewicz and Narkiewicz, 2008; Narkiewicz *et al.*, 2011, 2015). The estimated thickness of the eroded Devonian and Carboniferous strata is almost 3 km. The increase in subsidence in the Cretaceous did not impact on the thermal maturity of the basin infill. However, on the basis of recently published results by Krzywiec *et al.* (2018b), 1 km of eroded Jurassic–Triassic deposits was added, which allowed even better calibration of the model from scenario 2.

DISCUSSION

The structural seismic interpretation, combined with sequential restoration, provided new constraints on the Late Carboniferous Variscan thin-skinned structures, developed within the segment of the LB studied (Antonowicz *et al.*, 2003; Krzywiec *et al.*, 2017a, b; Tomaszczyk and Jarosiński, 2017). Analysis of the seismic image allowed the proposal of a kinematic model of structural evolution for the Late Carboniferous compressional structures. These Variscan structures were formed, owing to NE-directed tectonic compression and they detached within the Silurian fine-grained

shale complex. They are compressional structures that gradually diminish in throw towards the northeast, where uniformly dipping Carboniferous strata occur (Fig. 5). The lateral extent of Variscan deformations described in the northwestern part of the LB was controlled by the basement step in the KFZ, which played the role of buttress and was a site of strain localization during the Late Carboniferous compression. This basement high impeded the propagation of the shortening further to the northeast (Krzywiec *et al.*, 2017b). The basement step seems to be composed of fault segments, characterized by along-strike variations in fault throw. It seems that these fluctuations determined the position of the mushwad structure – the relatively high displacement (i.e. more than $\sim 1,700$ m) would prevent strain transmission to the northeast of the KFZ and development of the mushwad ahead of the basement step (Fig. 9). Lower fault offset would facilitate the transmission of shortening further to the northeast, although significant thickness reduction of the Silurian strata in the hanging wall of the KFZ resulted in the development of the mushwad directly above the basement step (Fig. 6; see also Krzywiec *et al.*, 2017b). Cross-section restoration also evidenced pre-Carboniferous basement KFZ activity, reflected in the Upper Devonian growth of strata above the KFZ (Fig. 7), as previously reported by other authors (e.g., Krzywiec, 2007; Narkiewicz *et al.*, 2007b; Narkiewicz, 2011; Krzywiec *et al.*, 2017b; Tomaszczyk and Jarosiński, 2017).

Analogue models of the brittle sedimentary cover shortened above the smooth basement surface suggest that variations in detachment layer thickness controlled the geometry of folds and thrusts (Cotton and Koyi, 2000; Costa and Vendeville, 2002). The shear strength of the tectonic wedge was a function of thickness of the decollement layer. Pinch-

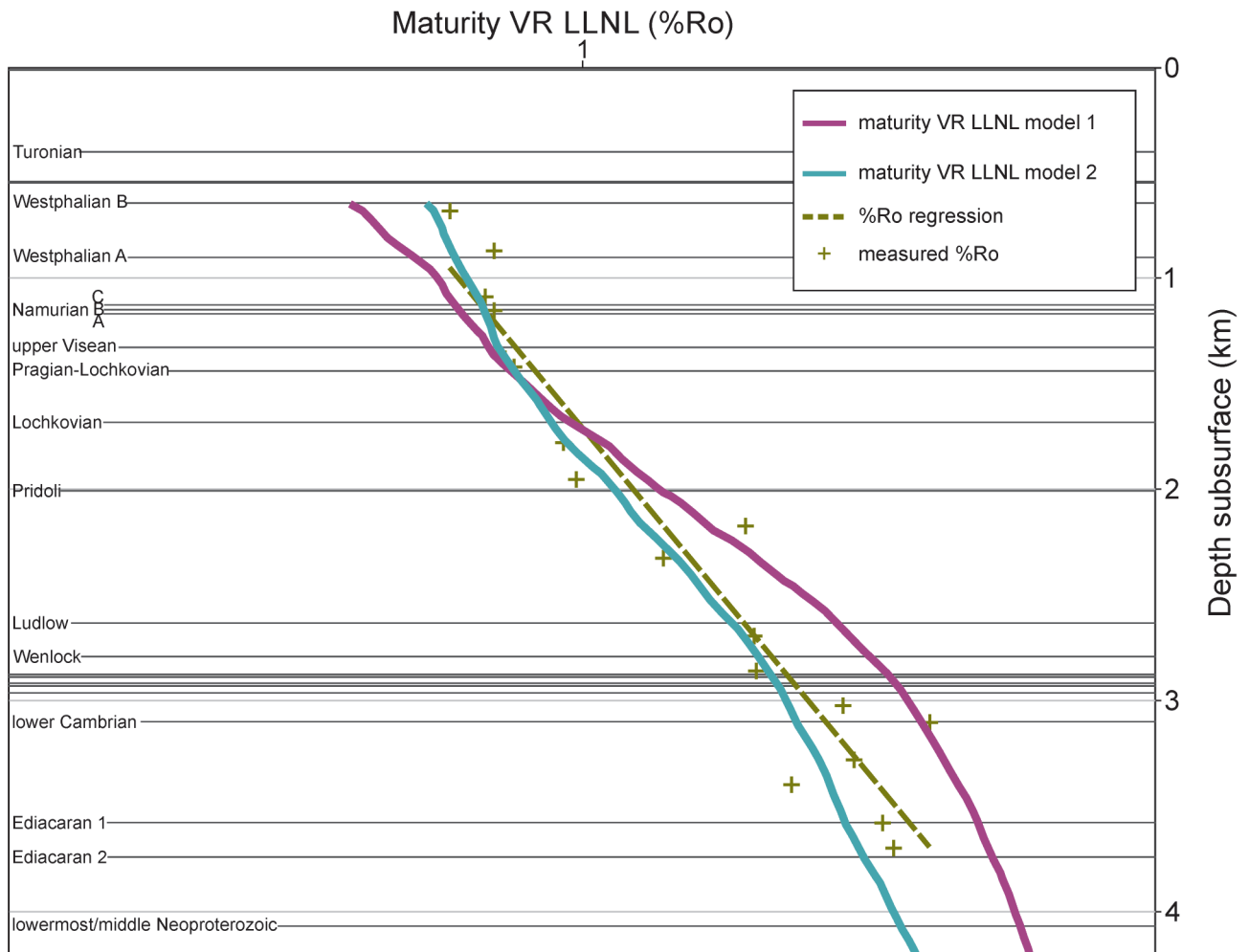


Fig. 13. Vitrinite reflectance calibration curves; green pluses-measured vitrinite reflectance data after Paczeńska (2007); scenario 1 calibration – pink line; scenario 2 calibration – blue line. Figure taken from Stypa *et al.* (2017).

ing out of the detachment layer caused a gradual transition from ductile to frictional behaviour; thus, thrust-fault propagation in the frontal part of the tectonic wedge required higher shear stress, compared to that in its internal portion. Sandbox experiments carried out by Smit *et al.* (2003) show that the box folds, fore- and backthrusts should be expected in areas characterized by a thick decollement. In contrast, a series of foreland-vergent thrust sheets forms, when the brittle sedimentary cover is shortened above a thin detachment layer (Smit *et al.*, 2003). In the southeastern part of the LB, no major basement step occurs and mostly SW-dipping forethrusts cut the Palaeozoic sedimentary cover (Fig. 5). The most plausible explanation for the structural geometry observed at the present day may be the pinching out of the Silurian strata to the NE that controls the extent of thin-skinned deformation. Additionally, the relatively small thickness of the ductile strata in this region, compared to the >2,000 m-thick Silurian rocks in the northwestern part of the LB, may explain the lateral variations in the vergence of the Late Palaeozoic structures.

The kinematic evolution of the high-angle thrusts may be characterized either as (1) pre-existing normal faults, which were reactivated during basin inversion; or (2) synsedimen-

tary Late Carboniferous reverse faults. The first scenario may explain the evolution of the foreland-vergent high-angle thrusts. These structures would originate during the Carboniferous as low-displacement, synsedimentary, normal faults. One such normal fault was interpreted on Figure 9 near the RKB/LB boundary. However, in the case of these inverted normal faults, the presence of a rollover anticline and growth strata – features that are typical for synsedimentary faults – are not observed. Basin inversion generated reverse offsets not exceeding 500 m. The structural evolution of the high-angle Miocene Carlsbad fault, inverted during the Pliocene–Holocene and reported by Rivero and Shaw (2011) may serve as an analogous structure for the Palaeozoic high-angle normal faults cutting the Carboniferous strata in the Lublin Basin. The alternative scenario implies Late Carboniferous thin-skinned thrust nucleation and synkinematic sedimentation. Following the results of sandbox modelling (Pichot and Nalpas, 2009; Wu and McClay, 2011; Barrier *et al.*, 2013), symmetrical fold growth and thrust propagation with dip angles ranging between 30° and 60°, is typical for thrust wedges, where the sedimentation-to-uplift ratio is not greater than 1. This model may explain the evolution of the thrusts, located in the southwestern part

of the LB, as vertical uplift along these faults attains up to 1,100 m and is equal to the average thickness of the missing Carboniferous strata (Fig. 9). However, owing to the erosion of the uppermost Carboniferous sedimentary sequence and the lack of growth strata, the selection of the most suitable model remains challenging.

Although the first-order Late Palaeozoic structures appear to be of compressional origin, it seems possible that they were overprinted in a strike-slip or oblique-slip regime, possibly during the latest stages of Variscan deformation, owing to the rotation of the maximum compression axis from NNE–SSW to WSW–ENE (Narkiewicz, 2007). This deformation mode is inferred using the results of core analysis of the Kock IG-1 well, where steeply-dipping fault planes are marked by numerous oblique slickensides (Fig. 14). The strike-slip reactivation of the major pre-existing structures seems to be unlikely, as an *en-echelon* fault array is expected to occur at an incipient stage of wrench faulting (Schlische *et al.*, 2002; Dooley and Schreurs, 2012). The lack of E–W or WNW–ESE-striking structures in the vicinity of the KFZ may suggest that the Variscan strike-slip reactivation of the basement fault may be an implausible scenario. Additionally, interpretation of the 3D seismic cube from the southeastern part of the LB did not provide evidences for any significant strike-slip faulting, as the faults reveal a uniform NW–SE trend (Fig. 15). Therefore, like Tomaszczyk and Jarosiński (2017), the present authors

concluded that distributed shear acted only locally and had a subordinate impact on the regional evolution of the LB.

The thin-skinned fault-related fold of the KFZ is cored by deformed Silurian strata. The lack of a clear seismic image and deep wells penetrating the Palaeozoic cover prompted numerous authors to discuss the deformation mode and internal structure in this zone (see e.g., Pelc, 1999; Krzywiec, 2009; Krzywiec *et al.*, 2017b; Tomaszczyk and Jarosiński, 2017). The lack of distinct seismic reflections within the fold core may be attributed either to a high dip angle of the strata, not imaged by seismic reflection data, or to a complex pattern of internal deformation. The present authors are inclined to support the second solution, as most probably seismic data would be able to image reflections from steeply dipping pre-Devonian layers, as in the case of the Devonian and Carboniferous strata (Fig. 6; Krzywiec *et al.*, 2017b). Abrupt thickening of the Silurian shales in the fold core may result from a ductile mode of strain accommodation, where the term ‘ductile’ refers to the sub-seismic-scale deformations, such as disharmonic folding, thrust faulting, distributed shear and cleavage formation. Late Devonian propagation of the high-angle basement fault through the entire sedimentary cover has been ruled out on the basis of the seismic interpretation of Kufraśa *et al.* (2018) from the southeastern termination of the KFZ, where fault offset was distributed in the triangular shear zone ahead of the fault tip and accommodated by folding of the Silurian–Devonian

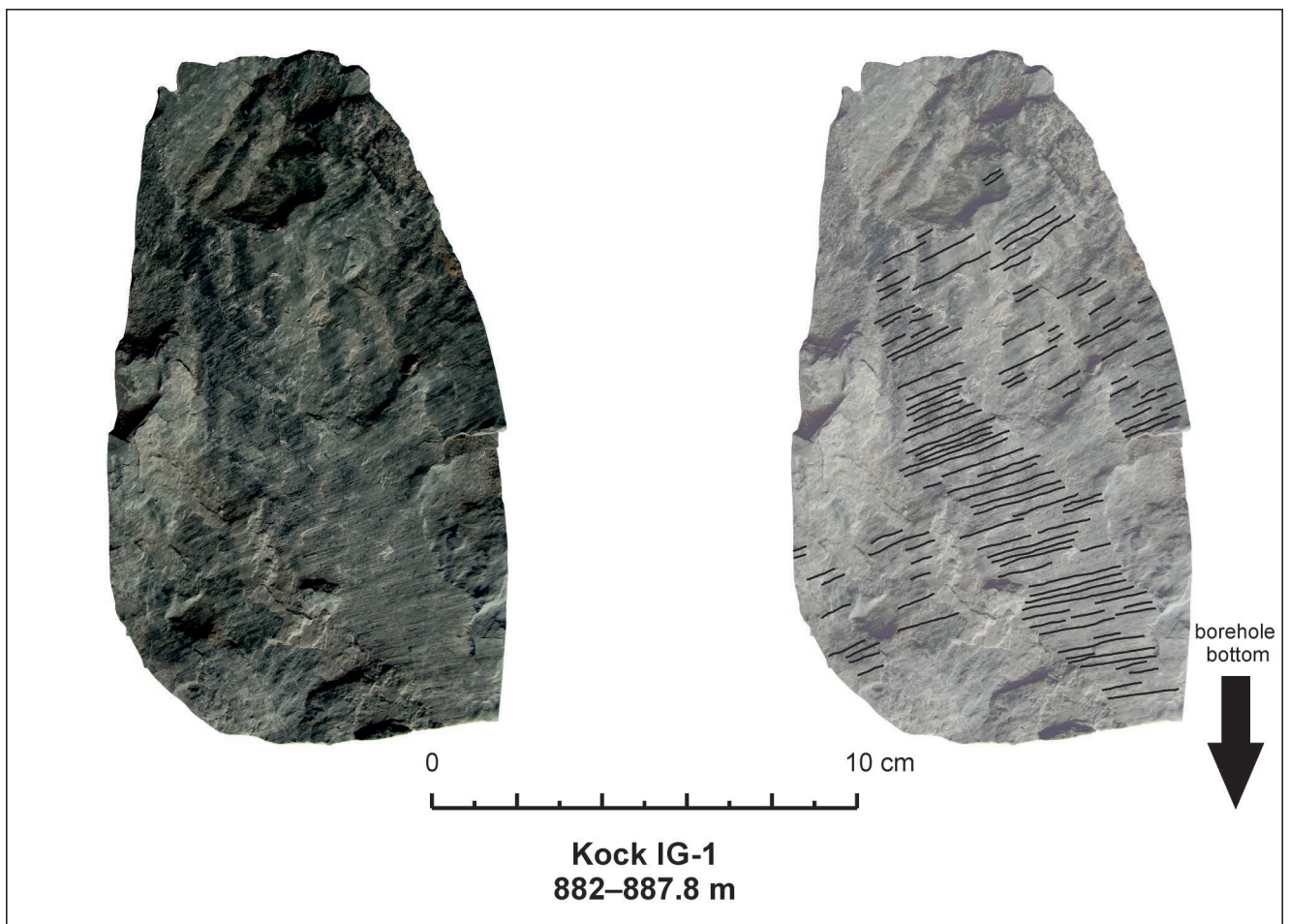


Fig. 14. Oblique-slip slickensides on the high-angle fault plane. The Kock IG-1 well, interval: 882–887.8 m (Silurian).

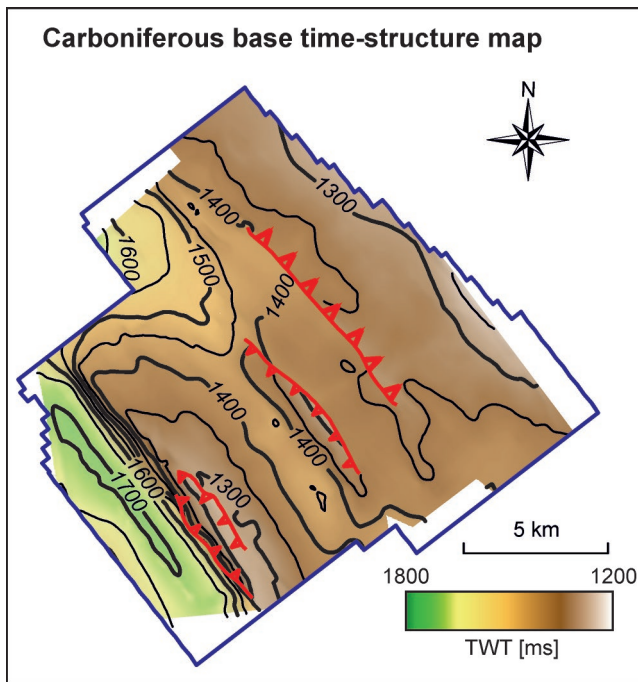


Fig. 15. Time structure map of the basal Carboniferous seismic horizon. Note the lack of an *en-echelon* fault array, indicative for a wrench tectonic regime.

sedimentary sequence. Broad zones of ductile deformation developed in the fine-grained rocks are termed ‘mushwads’ (malleable, unctuous shale, weak-layer accretion in a ductile duplex; Thomas, 2001, 2018). They were reported in the Appalachians, on the basis of outcrop, seismic and well studies, and are composed of strongly deformed Conasauga Cambrian shales (Thomas, 2007a, b; Pashin *et al.*, 2012). Mushwad structures form, when the sedimentary layer is shortened and detached along a thick decollement layer in front of a basement step. Core analysis of the Kock IG-1 well, which penetrated the Silurian strata in the KFZ, has revealed that the deformation pattern of densely fractured, crushed or folded shales (Fig. 16A, B) resembles that observed in the Appalachian mushwads (Fig. 16C–D). The idea of Late Carboniferous development of the mushwad structure in the KFZ (Krzywiec *et al.*, 2017b) partly corresponds to previously published concepts of thin-skinned deformation, focused above the basement step (Pelc, 1999; Krzywiec, 2009; Tomaszczyk and Jarosiński, 2017). Owing to presumably disharmonic folding, quantitative modelling of the KFZ remains challenging. The deformation pattern in the fold core is complex and the relationship between the strain amount accommodated in ductile and the overlying brittle strata is non-linear, as would be expected for classical fault-related folds and the structure analysed cannot be restored in a strict classical sense (Suppe, 2009).

The thickness of eroded Devonian strata, derived from published pre-deformation thickness reconstructions (Modliński, 2010) and included in cross-section restoration, agrees with the results of the subsidence modelling. However, in case of the Carboniferous sedimentary sequence, a major discrepancy is observed – the estimated Late- and post-

Late Carboniferous erosion, derived from the cross-section restoration, is ca. 3,000 m less than the number obtained in subsidence modelling. The reasons of this disagreement can be threefold: (1) the initial thickness reconstruction based on the maps of Modliński (2010) and included in the sequential restoration was not corrected for compaction, in contrast to the subsidence modelling of this study; (2) the multiple phases of Mesozoic uplift and erosion were not included in the cross-section restoration; and (3) the initial presence of the uppermost Carboniferous strata (uppermost Westphalian and/or Stephanian), which underwent Variscan erosion. The simple equation given by Van Hinte (1978) was employed to estimate roughly the effect of thickness reduction by compaction in the well selected for subsidence analysis. It relates present-day thickness and porosity measured in a given rock as follows:

$$T_0 = ((1-\phi_N) \cdot T_N) / (1-\phi_0)$$

where: T_0 - initial thickness, ϕ_0 - initial porosity, T_N - present-day thickness, and ϕ_N - present-day porosity. Assuming an initial porosity equal to 0.56 for shaly sandstone, which is the most appropriate for mixed sandstone-mudstone-shale Carboniferous strata (Allen and Allen, 2005), and taking the present-day thickness (791 m) and average porosity (0.072) of the Carboniferous sedimentary rocks in the Busówno IG-1 well (Paczeńska, 2007), the estimated initial thickness of the Carboniferous strata is ca. 1,607 m. This number is 816 m higher than the present-day thickness. Therefore, it is plausible to infer that the compaction reduced the initial thickness of the Carboniferous strata by ca. 800 m. The estimated correction for compaction reduces the discrepancy to ca. 2,200 m. It should be stressed that the estimate of total erosion based on subsidence modelling includes the results of recent investigations on multiple-phase Mesozoic uplift and erosion, which might have caused the removal of up to 1,000 m of the Mesozoic overburden (Krzywiec *et al.*, 2018b). Correction of the model discrepancy by the amount of Mesozoic erosion (1,000 m) results in a difference of 1,200 m between the values obtained from subsidence modelling and cross-section restoration. This value would be attributed to the missing portion of the Carboniferous sedimentary sequence. The estimates presented should be treated as tentative and used as a starting point for further research.

CONCLUSIONS

A new approach, integrating seismic and well data with structural restoration and subsidence analysis, resulted in an improved structural model of the Late Palaeozoic evolution of the Lublin Basin. The results presented in this paper focus on the key factors controlling thin-skinned Variscan Late Carboniferous deformation and on an attempt to estimate the amount of eroded uppermost Carboniferous strata.

Silurian shales played the role of a regional detachment level, above which the Devonian–Carboniferous sedimentary cover was shortened to create thin-skinned folds and thrusts. Second-order structures may be rooted in local detachments. High-angle thrusts may originate either as purely

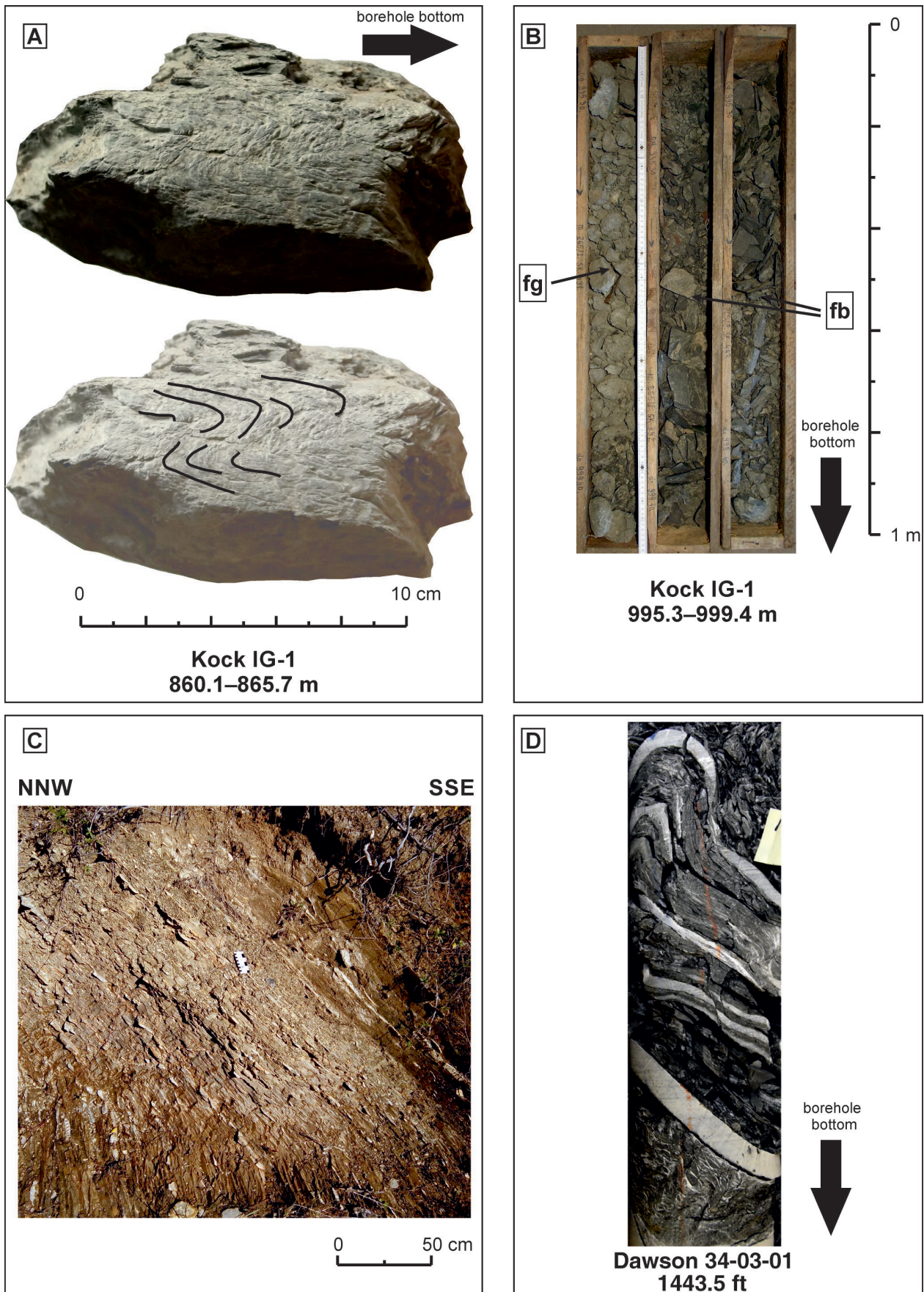


Fig. 16. Deformations in the Kock Fault Zone and the Conasauga shales in Alabama, USA. **A.** Examples of sub-seismic-scale Late Palaeozoic deformation observed in Silurian strata, Kock IG-1 well. **B.** Fault breccia (fb) and fault gauge (fg) in the Kock IG-1 well; arrow indicates core base. **C.** Outcrop view of the Middle–Upper Cambrian Conasauga Shale in the Gadsden mushwad near Pinedale Lake, St. Clair County, Alabama, USA. **D.** Small-scale deformation of the Conasauga Shale, Dawson 34-03-01 core (Pashin *et al.*, 2012).

compressional structures, or as inverted normal faults. The lateral extent of compressional deformation was controlled either by presence of a basement step, i.e. the Kock Fault Zone (northwestern part of the LB) or by gradual thickness reduction of the detachment level (SE part of the LB) that impeded the propagation of the shortening further to the NE.

The described fold-and-thrust deformations originated owing to the Late Carboniferous compressional stress field, although minor younger Late Palaeozoic strike-slip/oblique-slip reactivation can be inferred from the core-scale structures. Wrench tectonics acted only locally as distributed shear and did not significantly overprint the older compressional structures. Therefore, neglecting the strike-slip component of deformation during cross-section restoration seems not to introduce substantial error to the results obtained.

The basement step related to the KFZ acted in the Late Carboniferous as a region of contractional strain concentration. The internal structure of the thin-skinned anticline located above this basement step was interpreted as cored by a mushwad-type structure displaying a complex pattern of sub-seismic-scale ductile deformation. Along-strike variations in the fault throw seem to have controlled the position of the mushwad relative to the basement step. Surface outcrops of strongly deformed Conasauga shales in the Gadsden mushwad (Appalachians) are considered to be possible structural analogues of the KFZ.

Subsidence analysis carried out for the Busówno IG-1 well revealed that up to 3,400 m of Carboniferous and younger strata were removed during multiple Late Carboniferous and post-Late Carboniferous erosional events. This value should be treated as cumulative, taking into account the effect of compaction (~800 m), Mesozoic erosion (~1,000 m) and the missing portion of the Carboniferous sedimentary sequence (~1,200 m). Late Devonian–Early Carboniferous basement faulting was associated with localized deposition of Devonian growth strata at the footwall of the KFZ and at least 500 m of erosion at its hanging wall.

Acknowledgements

This research was in part carried out in the framework of the GAZGEOLMOD project, funded by the National Centre for Research and Development (NCBiR). Seismic and well data were kindly provided by the Polish Oil and Gas Company (PGNiG). The authors are indebted to IHS Markit, Petroleum Experts Ltd. and Platte River Associates for academic license for the Kingdom 2018, Midland Valley Move 2018, and BasinMod 2014 software, respectively. The authors would like to express their gratitude to the reviewers Andrea Artoni and Michał Krobicki for their thorough reviews and comments.

REFERENCES

- Allen, P. A. & Allen, J. R., 2005. *Basin Analysis: Principles and Applications. Second Edition*. Blackwell Publishing, Malden, 549 pp.
- Antonowicz, L., Hooper, R. & Iwanowska, E., 2003. Lublin Syncline as a result of thin-skinned Variscan deformation (SE Poland). *Przegląd Geologiczny*, 51: 344–350. [In Polish, English summary.]
- Antonowicz, L. & Iwanowska, E., 2004. Thin-skinned tectonics of the Lublin Basin. *Przegląd Geologiczny*, 52: 128–130. [In Polish.]
- Baldwin, B. & Butler, C. O., 1985. Compaction curves. *American Association of Petroleum Geologists Bulletin*, 69: 622–626.
- Barrier, L., Nalpas, T., Gapais, D. & Proust, J.-N., 2013. Impact of synkinematic sedimentation on the geometry and dynamics of compressive growth structures: insights from analogue modelling. *Tectonophysics*, 608: 737–752.
- BasinMod 2-D, 2019. BasinMod® 2-D. <https://www.platte.com/docman-files/fact-sheets/13-basinmod-2-d-1/file.html> [04.06.2019.]
- Bilowa, J., 1981. Identification of reflection seismic boundaries with the use of seismic well logs in the Terebiń area. *Geological Quarterly*, 25: 571–580. [In Polish, with English summary.]
- Bogdanova, S. V., Bingen, B., Gorbatshev, R., Kheraskova, T. N., Kozlov, V. I., Puchkov, V. N. & Volozh, Y. A., 2008. The East European Craton (Baltica) before and during the assembly of Rodinia. *Precambrian Research*, 160: 23–45.
- Botor, D., Kotarba, M. & Kosakowski, P., 2002. Petroleum generation in the Carboniferous strata of the Lublin Trough (Poland): an integrated geochemical and numerical modelling approach. *Organic Geochemistry*, 33: 461–476.
- Central Geological Database, 2019. Central Geological Database. <http://baza.pgi.gov.pl> [04.06.2019.]
- CGG, 2019. Geosoft Resources. <https://www.cgg.com/en/What-We-Do/GeoSoftware/GeoSoftware-Resources> [04.06.2019.]
- Costa, E. & Vendeville, B. C., 2002. Experimental insights on the geometry and kinematics of fold-and-thrust belts above weak, viscous evaporitic décollement. *Journal of Structural Geology*, 24: 1729–1739.
- Cotton, J. T. & Koyi, H., 2000. Modelling of thrust fronts above ductile and frictional detachments: Application to structures in the Salt Range and Potwar Plateau, Pakistan. *Geological Society of America Bulletin*, 112: 351–363.
- Dadlez, R., Narkiewicz, M., Stephenson, R. A., Visser, M. T. M & van Wess, J.-D., 1995. Tectonic evolution of the Mid-Polish Trough: modelling implications and significance for central European geology. *Tectonophysics*, 252: 179–195.
- Deep Time Maps, 2019. Deep Time Maps™, map of ancient Earth. <http://deeptimemaps.com/> [04.06.2019.]
- Dooley, T. P. & Schreurs, G., 2012. Analogue modelling of intraplate strike-slip tectonics: a review and new experimental results. *Tectonophysics*, 574–575: 1–71.
- Dziwińska, L. & Józwiak, W., 2000. Lithological variation of the Carboniferous data in the Lublin Trough in the light geophysical interpretation. *Biuletyn Państwowego Instytutu Geologicznego*, 392: 5–48. [In Polish, with English summary.]
- Gradstein, F. M., Ogg, J. G., Schmitz, M. D. & Ogg, G. M. (eds), 2012. *The Geological Time Scale 2012*. Elsevier, Amsterdam-Boston, 1176 pp.
- Kaczyński, J., 1984. Perspektywy ropogazoności Lubelszczyzny. *Przegląd Geologiczny*, 32: 330–333. [In Polish.]
- IHS Kingdom, 2019. Documentation (PDF versions). http://productdownloads.ihs.com/Documentation/Kingdom/2018/KingdomDocuments_2018.zip [04.06.2019.]
- Krzywiec, P., 2007. Nowe spojrzenie na tektonikę regionu lubelskiego (SE Polska) oparte na wynikach interpretacji danych sejsmicznych. *Biuletyn Państwowego Instytutu Geologicznego*, 422: 1–18. [In Polish, with English summary.]

- Krzywiec, P., 2009. Devonian–Cretaceous repeated subsidence and uplift along the Teisseyre–Tornquist zone in SE Poland – insight from seismic data interpretation. *Tectonophysics*, 475: 142–159.
- Krzywiec, P., Gągała, Ł., Mazur, S., Słonka, Ł., Kufraś, M., Malinowski, M., Pietsch, K. & Golonka, J., 2017a. Variscan deformation along the Teisseyre–Tornquist Zone in SE Poland: thick-skinned structural inheritance or thin-skinned thrusting? *Tectonophysics*, 718: 83–91.
- Krzywiec, P., Gutowski, J., Walaszczyk, I., Wróbel, G. & Wybraniec, S., 2009. Tectonostratigraphic model of the Late Cretaceous inversion along the Nowe Miasto–Zawichost Fault Zone, SE Mid-Polish Trough. *Geological Quarterly*, 53: 27–48.
- Krzywiec, P., Mazur, S., Gągała, Ł., Kufraś, M., Lewandowski, M., Malinowski, M. & Buffenmyer, V., 2017b. Late Carboniferous thin-skinned compressional deformation above the SW edge of the East European craton as revealed by seismic reflection and potential field data – Correlations with the Variscides and the Appalachians. *The Geological Society of America Memoir*, 213: 353–372.
- Krzywiec, P., Poprawa, P., Mikołajczak, M., Mazur, S. & Malinowski, M., 2018a. Deeply concealed half-graben at the SW margin of the East European Craton (SE Poland) – evidence for Neoproterozoic rifting prior to the break-up of Rodinia. *Journal of Paleogeography*, 7: 88–97.
- Krzywiec, P., Stachowska, A. & Stypa, A., 2018b. The only way is up – on Mesozoic uplifts and basin inversion events in SE Poland. In: Kilhams, B., Kukla, P. A., Mazur, S., McKie, T., Mijndieff, H. F. & van Ojik, K. (eds), *Mesozoic Resource Potential in the Southern Permian Basin*. Geological Society, London, Special Publications, 469: 33–57.
- Kufraś, M., Krzywiec, P. & Słonka, Ł., 2017. Model paleozoicznej ewolucji tektonicznej SE Polski (blok radomsko-kraśnicki i basen lubelski) w oparciu o wyniki interpretacji danych sejsmicznych. In: Golonka, J. & Bębenek, S. (eds), *Opracowanie map zasięgu, biostratygrafia utworów dolnego paleozoiku oraz analiza ewolucji tektonicznej przykrawędziowej strefy platformy wschodnioeuropejskiej dla oceny rozmieszczenia niekonwencjonalnych złóż węglowodorów*. Arka, pp. 337–355. [In Polish.]
- Kufraś, M., Słonka, Ł., Krzywiec, P., Dzwiniel, K. & Zacharski, J., 2018. Fracture pattern of the Lower Paleozoic sedimentary cover in the Lublin Basin of southeastern Poland derived from seismic attribute analysis and structural restoration. *Interpretation*, 6: SH73–SH89.
- Kuszniir, N. J., Stovba, S. M., Stephenson, R. A. & Poplavskii, K. N., 1996. The formation of the northwestern Dniepr-Donets Basin: 2-D forward and reverse syn-rift and post-rift modeling. *Tectonophysics*, 268: 237–255.
- Mazur, S., Gągała, Ł., Kufraś, M. & Krzywiec, P., 2018. Application of two-dimensional gravity models as input parameters to balanced cross-sections across the margin of the East European Craton in SE Poland. *Journal of Structural Geology*, 116: 223–233.
- Mazur, S., Mikołajczak, M., Krzywiec, P., Malinowski, M., Lewandowski, M. & Buffenmyer, V., 2016. Pomeranian Caledonides, NW Poland – a collisional suture or thin-skinned fold-and-thrust belt? *Tectonophysics*, 692: 29–43.
- Modliński, Z. (ed.), 2010. *Paleogeological atlas of the sub-Permian Paleozoic of the East-European Craton in Poland and neighbouring areas*. Polish Geological Institute, Warsaw.
- Move, 2019. Move Documentation. <https://www.mve.com/resources/move-documentation> [04.06.2019.]
- Narkiewicz, M., 2003. Tektoniczne uwarunkowania rowu lubelskiego (dewon–karbon). *Przegląd Geologiczny*, 51: 771–776. [In Polish, with English summary.]
- Narkiewicz, M., 2007. Development and inversion of Devonian and Carboniferous basins in the eastern part of the Variscan foreland (Poland). *Geological Quarterly*, 51: 231–256.
- Narkiewicz, M., 2011. Lithostratigraphy, depositional systems and transgressive-regressive cycles in the Devonian of the Lublin Basin (south-eastern Poland). *Prace Państwowego Instytutu Geologicznego*, 196: 53–146. [In Polish, with English summary.]
- Narkiewicz, M., Jarosiński, M. & Krzywiec, P., 2007a. Diagenetic and tectonic processes controlling reservoir properties of the Frasnian dolostones in the central part of the Lublin Graben (Eastern Poland). *Przegląd Geologiczny*, 55: 61–70. [In Polish, with English summary.]
- Narkiewicz, M., Jarosiński, M., Krzywiec, P. & Waksmundzka, M. I., 2007b. Regionalne uwarunkowania rozwoju i inwersji basenu lubelskiego w dewonie i karbonie. *Biuletyn Państwowego Instytutu Geologicznego*, 422: 19–34. [In Polish, with English summary.]
- Narkiewicz, M., Maksym, A., Malinowski, M., Grad, M., Guterch, A., Petecki, Z., Probulski, J., Janik, T., Majdański, M., Środa, P., Czuba, W., Gaczyński, E. & Jankowski, L., 2015. Transcurrent nature of the Teisseyre–Tornquist Zone in Central Europe: results of the POLCRUST-01 deep reflection seismic profile. *International Journal of Earth Sciences*, 104: 775–796.
- Narkiewicz, M. & Narkiewicz, K., 2008. The mid-Frasnian subsidence pulse in the Lublin Basin (SE Poland): sedimentary record, conodont biostratigraphy and regional significance. *Acta Geologica Polonica*, 58: 287–301.
- Narkiewicz, M., Narkiewicz, K. & Turnau, E., 2011. Rozwój sedymentacji dewońskiej w basenie łysogórsko-radomskim i lubelskim. *Prace Państwowego Instytutu Geologicznego*, 196: 289–318. [In Polish, with English summary.]
- Nikishin, A., Ziegler, P., Stephenson, R., Cloetingh, S., Furne, A., Fokin, P., Ershov, A., Bolotov, S., Korotaev, M., Alekseev, A., Gorbachev, V., Shipilov, E., Lankreijer, A., Bembinova, E. & Shalimov, I., 1996. Late Precambrian to Triassic history of the East European Craton: dynamics of sedimentary basin evolution. *Tectonophysics*, 268: 23–63.
- Paczeńska, J., 2006. Evolution of late Neoproterozoic rift depocentres and facies in the Lublin–Podlasie sedimentary basin. *Prace Państwowego Instytutu Geologicznego*, 186: 1–29. [In Polish, with English summary.]
- Paczeńska, J., 2010. The evolution of late Ediacaran riverine-estuarine system in the Lublin–Podlasie slope of the East European Craton, southeastern Poland. *Polish Geological Institute Special Papers*, 27: 1–96.
- Paczeńska, J., 2014. Lithostratigraphy of the Ediacaran deposits in the Lublin–Podlasie sedimentary basin (eastern and south-eastern Poland). *Biuletyn Państwowego Instytutu Geologicznego*, 460: 1–24. [In Polish, with English summary.]
- Paczeńska, J. (ed.), 2007. *Profil Głębokich Otworów Wiertniczych PIG – Busówno IG-1*. Państwowy Instytut Geologiczny, Warszawa, 218 pp. [In Polish, with English summary.]
- Pashin, J. C., Kopaska-Merkel, D. C., Arnold, A. C., McIntyre, M. R. & Thomas, W. A., 2012. Gigantic, gaseous mushwads in Cam-

- brian shale: Conasauga Formation, southern Appalachians, USA. *International Journal of Coal Geology*, 103: 70–91.
- Pelc, T., 1999. Dewońsko-karboński diapiryzm sylurskich utworów ilastych basenu lubelskiego. *Geofizyka w geologii, górnictwie i ochronie środowiska*. V Konferencja Naukowo-Techniczna, Kraków, 137–142. [In Polish.]
- Pepel, A., 1974. Reflectors as established by vertical seismic profiling in the northern and central part of the Lublin Graben. *Geological Quarterly*, 18: 850–864.
- Pharaoh, T. C., Dugar, M., Geluk, M. C., Kockel, F., Krawczyk, C. M., Krzywiec, P., Scheck–Wenderoth, M., Thybo, H., Vejbaek, O. V. & van Wees, J.-D., 2010. Tectonic evolution. In: Doornbal, J. C. & Stevenson, A. G. (eds), *Petroleum Geological Atlas of the Southern Permian Basin Area*. EAGE Publications b.v., Houten, pp. 25–57.
- Pichot, T. & Nalpas, T., 2009. Influence of synkinematic sedimentation in a thrust system with two decollement levels; analogue modelling. *Tectonophysics*, 473: 466–475.
- Poprawa, P., 2006a. Neoproterozoic break-up of the supercontinent Rodinia/Pannotia recorded by development of sedimentary basins at the western slope of Baltica. *Prace Państwowego Instytutu Geologicznego*, 186: 165–188. [In Polish, with English summary.]
- Poprawa, P., 2006b. Development of the Caledonian collision zone along the western margin of Baltica and its relation to the foreland basin. *Prace Państwowego Instytutu Geologicznego*, 186: 189–214. [In Polish, with English summary.]
- Pozaryski, W. & Dembowski, Z., 1983. *Geological Map of Poland and Neighboring Countries without Cenozoic, Mesozoic and Permian Deposits, 1:1000000*. Geological Institute, Warsaw. [In Polish.]
- Remin, Z., Gruszczynski, M. & Marshall, J. D., 2016. Changes in paleo-circulation and the distribution of ammonite faunas at the Coniacian–Santonian transition in central Poland and western Ukraine. *Acta Geologica Polonica*, 66: 107–124.
- Rivero, C. & Shaw, J. H., 2011. Active folding and blind thrust faulting induced by basin inversion processes, Inner California Borderlands. In: Shaw, J. & Suppe, J. (eds), *Thrust fault-related folding*. American Association of Petroleum Geologists Memoir, 94: 187–214.
- Scheck–Wenderoth, M., Krzywiec, P., Zülke, R., Maystrenko, Y. & Frizheim, N., 2008. Permian to Cretaceous tectonics. In: McCann, T. (ed.), *The Geology of Central Europe. Volume II: Mesozoic and Cenozoic*. Geological Society, London, pp. 999–1030.
- Schlische, R. W., Withjack, M. O. & Eisenstadt, G., 2002. An experimental study of the secondary deformation produced by oblique-slip normal faulting. *American Association of Petroleum Geologists Bulletin*, 86: 885–906.
- Schmid, S. M., Bernoulli, D., Fügenschuh, B., Matenco, L., Schefer, S., Schuster, R., Tischler, M. & Ustaszewski, K., 2008. The Alpine-Carpathian-Dinaridic orogenic system: correlation and evolution of tectonic units. *Swiss Journal of Geosciences*, 101: 139–183.
- Smit, J. H.W., Brun, J. P. & Sokoutis, D., 2003. Deformation of brittle-ductile thrust wedges in experiments and nature. *Journal of Geophysical Research*, 108: 2480.
- Stampfli, G. M., Hochard, C., Verard, C., Wilhem, C. & von Raumer, J., 2013. The formation of Pangea. *Tectonophysics*, 593: 1–19.
- Stephenson, R. A., Narkiewicz, M., Dadlez, R., van Wees, J.-D. & Andriessen, P., 2003. Tectonic subsidence modelling of the Polish Basin in the light of new data on crustal structure and magnitude of inversion. *Sedimentary Geology*, 156: 59–70.
- Stovba, S. M. & Stephenson, R. A., 1999. The Donbas Foldbelt: its relationships with the uninverted Donets segment of the Dniepr–Donets Basin, Ukraine. *Tectonophysics*, 313: 59–83.
- Stypa, A., Krzywiec, P., Kufrasa, M. & Słonka, Ł., 2017. Analiza krzywych subsydencji tektonicznej na obszarze basenu lubelskiego. In: Golonka, J. & Bębenek, S. (eds), *Opracowanie map zasięgu, biostratygrafia utworów dolnego paleozoiku oraz analiza ewolucji tektonicznej przykrawędziowej strefy platformy wschodnioeuropejskiej dla oceny rozmieszczenia niekonwencjonalnych złóż węglowodorów*. Arka, Cieszyn, pp. 372–380. [In Polish.]
- Suppe, J., 2009. Mass balance and thrusting in detachment fold. *American Association of Petroleum Geologists Memoir*, 94: 1–16.
- Thomas, W. A., 2001. Mushwad: Ductile duplex in the Appalachian thrust belt in Alabama. *American Association of Petroleum Geologists Bulletin*, 85: 1847–1869.
- Thomas, W. A., 2007a. Balancing tectonic shortening in contrasting deformation styles through a mechanically heterogeneous stratigraphic succession. *Geological Society of America Special Paper*, 433: 227–290.
- Thomas, W. A., 2007b. Role of the Birmingham Basement Fault in thin-skinned thrusting of the Birmingham Anticlinorium, Appalachian Thrust Belt in Alabama. *American Journal of Science*, 307: 46–62.
- Thomas, W. A., 2018 (in press). Evolution of the concept and structure of a MUSHWAD. *Journal of Structural Geology*. Doi: <https://doi.org/10.1016/j.jsg.2018.05.001>.
- Tomaszczyk, M., 2015. *Ewolucja tektoniczna centralnej części basenu lubelskiego*. Unpublished PhD Dissertation, Polish Geological Institute, 129 pp. [In Polish.]
- Tomaszczyk, M. & Jarosiński, M., 2017. The Kock Fault Zone as an indicator of tectonic stress regime changes at the margin of the East European Craton (Poland). *Geological Quarterly*, 61: 908–925.
- Van Hinte, J. E., 1978. Geohistory analysis – application of micro-paleontology in exploration geology. *American Association of Petroleum Geologists Bulletin*, 62: 201–222.
- Woodward, N. B., Boyer, S. E. & Suppe, J. (eds), 1989. *Balanced Geological Cross-Sections: An Essential Technique in Geological Research and Exploration. Short Course in Geology* 6: 132 pp. AGU, Washington, D.C.
- Wu, J.E. & McClay, K.R., 2011. Two-dimensional analog modeling of fold and thrust belts: Dynamic interactions with syncontractional sedimentation and erosion. In: Shaw, J. & Suppe, J. (eds), *Thrust fault-related folding*. American Association of Petroleum Geologists Memoir, 94: 301–333.
- Ziegler, P. A. 1990. *Geological Atlas of Western and Central Europe, 2nd Edition*. Shell International Petroleum Maatschappij B.V. and Geological Society Publishing House, Bath, 239 pp.